Event-based Stabilization of Periodic Orbits for Underactuated 3D Bipedal Robots with Left-Right Symmetry

Kaveh Akbari Hamed and J. W. Grizzle, *Fellow, IEEE*

***Abstract*—Models of robotic bipedal walking are hybrid, with a differential equation describing the stance phase and a discrete map describing the impact event, that is, the non-stance leg contacting the walking surface. The feedback controllers for these systems can be hybrid as well, including both continuous and discrete (event-based) actions. This paper concentrates on the event-based portion of the feedback design problem for 3D bipedal walking. The results are developed in the context of robustly stabilizing periodic orbits for a simulation model of ATRIAS 2.1, a highly underactuated 3D bipedal robot with series-compliant actuators and point feet, against external disturbances as well as parametric and nonparametric uncertainty. It is shown that left-right symmetry of the model can be used to both simplify and improve the design of event-based controllers. Here, the event-based control is developed on the basis of the Poincaré map, linear matrix inequalities (LMIs), and robust optimal control (ROC). The results are illustrated by designing a controller that enhances the lateral stability of ATRIAS 2.1.**

I. Introduction

THE MAIN objective of this paper is to present a time-invariant and event-based control scheme for robust stabilization of periodic orbits for 3D bipedal walking in the presence of external disturbances as well as parametric and nonparametric uncertainty. The results are developed and illustrated on a simulation model of ATRIAS[1] 2.1 [1], [2] a highly underactuated 3D bipedal robot with point feet and series-compliant actuators (see Fig. 1). During the single support phase, the robot has 13 degrees of freedom (DOF) and 7 degrees of underactuation (DOU). Bipedal walking can be modeled as a system with impulse effects [3]- [18], which is a special class of hybrid systems. Steady-state walking locomotion corresponds to a periodic orbit in the model.

The most basic tool to investigate the stability of periodic orbits for hybrid systems is the method of Poincaré sections which replaces the flow of hybrid systems with a discrete-time system given by the Poincaré return map, which maps the evolution of the system's state from a point on a hyperplane transversal to the periodic orbit (called the Poincaré section [19]- [21]) back to the hyperplane [5]. If the continuous dynamics of the hybrid model depend on a set of adjustable parameters, the approach of Poincaré sections can also be used to design stabilizing feedback controllers for periodic orbits of the hybrid models [22], [23]. In particular, the parameters can be updated by an event-based controller when trajectories cross the Poincaré section. References [24]- [28] designed linear event-based controllers for stabilization of periodic walking and running on the basis of Jacobian linearizations for the corresponding Poincaré return maps. However, there are important problems when extending this approach to 3D bipedal robots with high degrees of underactuation and/or compliant elements, such as ATRIAS. The Poincaré return maps for 3D walking and running consist of two steps, that is, the mapping from right stance, to left stance, and back to right stance (or the opposite order), which we write informally as

$$x_{k+2} = P_{\mathrm{R}\to\mathrm{R}}(x_k, \beta_k).$$

An event-based controller designed on this representation changes the parameter β in a two-step manner, that is once per two steps as in [26]- [28]. Alternatively, the Poincaré map can be "factored" as

$$x_{k+2} = P_{\mathrm{L}\to\mathrm{R}}(x_{k+1}, \beta_{k+1}), \quad x_{k+1} = P_{\mathrm{R}\to\mathrm{L}}(x_k, \beta_k),$$

making explicit both leg transitions, in which case the parameter β can be now updated in a one-step manner, that is at each step. However, the discrete model arising in this case is periodically time-varying with period-2 [28], making the controller design problem more challenging.

A second issue is the wide range of time scales in the continuous dynamics, arising from the large springs in the series-compliant actuators, the relatively heavy body, and the light legs, which together render the robot's dynamics numerically stiff. This stiffness leads to uncertainty when the Jacobians of the Poincaré map are calculated using numerical differentiation algorithms such as two point symmetric differences or least squares, both of which are sensitive to the perturbation values used during calculation. Additional uncertainty arises when either external disturbances act on the robot's dynamics (e.g., pushing the robot) or parametric and nonparametric uncertainties are present in the model. In all of these cases, the evolution of the system on the Poincaré section is uncertain.

To overcome the above challenges, this paper proposes a time-invariant one-step hybrid control scheme on the basis of right-left symmetry, linear matrix inequalities (LMIs), and robust optimal control (ROC). The continuous-time portion of the hybrid controller employs a general class of time-invariant and nonlinear feedback laws to interact with the bipedal

K. Akbari Hamed was supported by DARPA Contract W91CRB-11-1-0002 and J. W. Grizzle was supported by NSF grant ECCS-1231171.

K. Akbari Hamed (**Corresponding Author**) and J. W. Grizzle are with the Electrical Engineering and Computer Science Department of the University Michigan, Ann Arbor, MI, USA, {kavehah,grizzle}@umich.edu

[1]The name is an acronym which stands for Assume The Robot Is A Sphere.

robot in both the sagittal and frontal planes. These feedback laws are assumed piecewise continuously differentiable; it is further assumed that they are parameterized by a set of finite-dimensional parameters referred to as the stabilizing parameters. It is shown how symmetry leads to the ability to design a general class of time-invariant one-step event-based controllers. To robustly stabilize desired walking gaits, the one-step event-based controller consists of two loops. The first loop, referred to as the robust stabilizer, introduces an LMI-based static update law for the Poincaré maps designed to be robust against numerical and parametric uncertainties. The second loop of the discrete action aims to increase the basin of attraction and robustness of the closed-loop system against parametric uncertainty and to reject external disturbances acting on the robot. In particular, the second loop, referred to as the ROC, updates the parameters of the continuous-time feedback laws by solving a min-max problem to optimize the worst case performance, while considering the saturation of the discrete-time controller for all possible disturbances and polyhedral parametric uncertainties in the Poincaré return maps. All of these results are illustrated on a simulation model of ATRIAS 2.1.

The paper also extends the analytical results to feedback laws arising from virtual constraints and hybrid zero dynamics (HZD) as special members of this general class. Virtual constraints are a set of holonomic constraints, defined as output functions in the configuration space of the mechanical system, used to coordinate the links of the robot and thereby to reduce the dimension of the system. These constraints are asymptotically satisfied through the action of a feedback controller within the step. They have been employed for planar [5], [6, Chap.5] and rigid 3D bipedal robots [8], [26], [28], and a rigid 3D monopedal runner [27]. One part of the LMI results was already presented in [29] for two-step event-based update laws. This paper adds the symmetry in the hybrid model, continuous-time feedback laws, Poincaré maps and corresponding Jacobian matrices to present a general class of one-step correction laws. Next, it extends the LMI stabilization for the one-step laws and adds the ROC formalism to increase the basin of attraction and to reject external disturbances. In addition, it extends the results to the HZD hybrid controller.

This paper is organized as follows. Section II presents the Lagrangian and impact models for ATRIAS. Section III addresses the symmetry between the right and left stance phases. Section IV presents the proposed nonlinear hybrid control strategy on the basis of one-step event-based update laws. In Section V, a robust one-step event-based update law is presented on the basis of LMI and ROC. It also addresses the push recovery and robust stabilization issues. Section VI extends the analytical results to feedback laws, arising from the virtual constraints. Section VII presents detailed numerical simulations to confirm the analytical results. Section VIII contains concluding remarks.

II. Hybrid Model of 3D Walking

The evolution of the mechanical system during 3D walking can be expressed by a *hybrid system* composed of two *continuous phases* to represent the right and left stance phases,

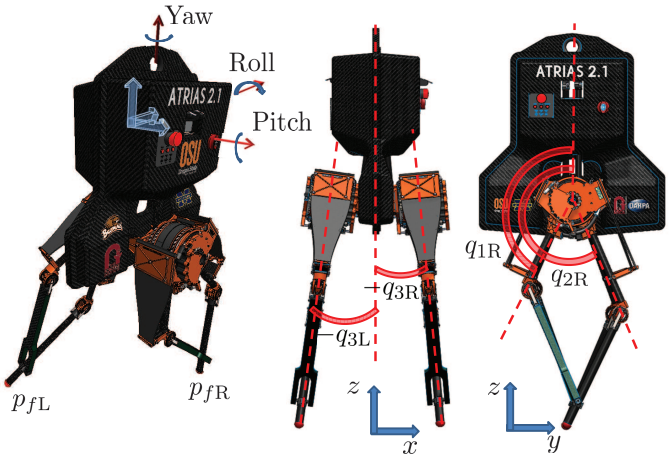

Fig. 1: ATRIAS 2.1, an underactuated 3D bipedal robot with series-compliant actuators and point feet. The isometric (left), back (middle) and side (right) views are shown with the associated configuration variables.

and two *discrete transitions* between the continuous phases to model the right-to-left and left-to-right transitions given by the impact of the non-stance legs [30]. The *double support phase*, corresponding to both legs being on the ground during impact, is assumed to be instantaneous.

A. Basic definitions

This section presents basic definitions to describe the hybrid model of walking by ATRIAS. To achieve this goal, a convenient set of configuration variables is chosen. During the single support phase, the mechanical system has 13 DOF. In particular, assume that $o_0x_0y_0z_0$ is an inertial frame attached to the ground which is referred to as the *world frame*. Next, attach the *torso frame* $o_{\mathrm{T}}x_{\mathrm{T}}y_{\mathrm{T}}z_{\mathrm{T}}$ to the torso link with the origin at its base. The orientation of the torso frame with respect to the world frame can be expressed by the rotation matrix $R^0_{\mathrm{T}} \in \mathrm{SO}(3)$ as

$$R^0_{\mathrm{T}} := R_z(q_{z\mathrm{T}})\, R_y(q_{y\mathrm{T}})\, R_x(q_{x\mathrm{T}}),$$

where R_x, R_y and R_z represent the basic rotations about the x, y and z axes, respectively. Moreover, $q_{z\mathrm{T}}$, $q_{y\mathrm{T}}$ and $q_{x\mathrm{T}}$ are referred to as the *yaw*, *roll* and *pitch* angles. According to Fig. 1, the angles of the right and left hips relative to the torso frame are denoted by $q_{3\mathrm{R}}$ and $q_{3\mathrm{L}}$, respectively. In addition, the angles of the shin and thigh links relative to the torso are represented by $q_{1\mathrm{R}}$ and $q_{2\mathrm{R}}$ for the right leg, and $q_{1\mathrm{L}}$ and $q_{2\mathrm{L}}$ for the left leg (see once again Fig. 1). We note that since the four-bar linkage of the leg structure forms a parallelogram, it consists of two pairs of parallel links and hence $q_{1\mathrm{R}}$ and $q_{1\mathrm{L}}$ denote the angles of the shin links with respect to the torso frame. The hip motors are connected to the body through fixed gear ratios and we denote their torques by $u_{3\mathrm{R}}$ and $u_{3\mathrm{L}}$. Consequently, the angles of the hip motors can be determined based on $q_{3\mathrm{R}}$ and $q_{3\mathrm{L}}$. On the other hand, the motors driving the legs in the sagittal plane are connected through *springs* (i.e., series-elastic actuators). For each of these motors, the angle of the output shaft of the harmonic drive is represented

by the subscript "gr". In particular, we introduce $q_{gr1\mathrm{R}}$, $q_{gr2\mathrm{R}}$, $q_{gr1\mathrm{L}}$, and $q_{gr2\mathrm{L}}$. Furthermore, $u_{1\mathrm{R}}$, $u_{2\mathrm{R}}$, $u_{1\mathrm{L}}$ and $u_{2\mathrm{L}}$ denote the torques generated by the corresponding motors. Finally, the generalized coordinates of the mechanical system during the right and left stance phases can be expressed as

$$q := (q_{z\mathrm{T}}, q_{y\mathrm{T}}, q_{x\mathrm{T}}, q_{1\mathrm{R}}, q_{2\mathrm{R}}, q_{1\mathrm{L}}, q_{2\mathrm{L}}, q_{gr1\mathrm{R}}, q_{gr2\mathrm{R}}, q_{3\mathrm{R}}, q_{gr1\mathrm{L}}, q_{gr2\mathrm{L}}, q_{3\mathrm{L}})' \in \mathcal{Q},$$

in which $\mathcal{Q}$ is the *configuration space* related to physically feasible configurations and prime represents matrix transpose. We note that the first seven components of q are unactuated whereas the remaining six components are actuated. The state vector of the system is defined as $x := (q', \dot{q}')' \in \mathcal{X} \subset \mathbb{R}^{26}$, where $\mathcal{X}$ is the *state manifold* taken as the *tangent bundle* of $\mathcal{Q}$, i.e., $\mathcal{X} := T\mathcal{Q} := \{(q', \dot{q}')' | \, q \in \mathcal{Q}, \dot{q} \in \mathbb{R}^{13}\}$. Furthermore, $u := (u_{1\mathrm{R}}, u_{2\mathrm{R}}, u_{3\mathrm{R}}, u_{1\mathrm{L}}, u_{2\mathrm{L}}, u_{3\mathrm{L}})' \in \mathcal{U}$ denotes the torque input, where $\mathcal{U} \subset \mathbb{R}^6$ is the set of admissible control inputs.

Throughout this paper, the subscripts "R" and "L" stand for right and left, respectively. In addition, the subscripts "R $\to$ L" and "L $\to$ R" will be used to represent the right-to-left and left-to-right impact maps. According to Fig 1, let $p_{f\mathrm{R}} := (p^x_{f\mathrm{R}}, p^y_{f\mathrm{R}}, p^z_{f\mathrm{R}})' \in \mathbb{R}^3$ and $p_{f\mathrm{L}} := (p^x_{f\mathrm{L}}, p^y_{f\mathrm{L}}, p^z_{f\mathrm{L}})' \in \mathbb{R}^3$ denote the Cartesian coordinates of the right and left point feet with respect to the world frame, where the subscripts "fR" and "fL" denote the right and left feet, respectively. Next, the *right-to-left switching manifold* can be defined as $\mathcal{S}_{\mathrm{R}\to\mathrm{L}} := \{(q', \dot{q}')' \in T\mathcal{Q} | \, p^z_{f\mathrm{L}}(q) = 0\}$, on which the right-to-left impact occurs during walking on flat ground. In an analogous manner, we can define $\mathcal{S}_{\mathrm{L}\to\mathrm{R}} := \{(q', \dot{q}')' \in T\mathcal{Q} | \, p^z_{f\mathrm{R}}(q) = 0\}$ as the *left-to-right switching manifold*.

B. Single support phase

The evolution of the mechanical system during the single support phase can be expressed by

$$D(q)\,\ddot{q} + H(q, \dot{q}) = B\,u, \tag{1}$$

in which $D(q) \in \mathbb{R}^{13\times13}$ denotes the positive-definite mass-inertia matrix and $B \in \mathbb{R}^{13\times6}$ represents the input matrix with the property $\operatorname{rank} B = \dim \mathcal{U} = 6$. Moreover, the vector $H(q, \dot{q})$ in (1) contains the Coriolis and centrifugal terms, the gravity vector, and the spring-damper forces arising from the compliant elements. In particular,

$$H(q, \dot{q}) := C(q, \dot{q})\,\dot{q} + G(q) + K_{\text{spring}}\,q + K_{\text{damper}}\,\dot{q}, \tag{2}$$

where $C(q, \dot{q})\,\dot{q} \in \mathbb{R}^{13}$ contains the Coriolis and centrifugal terms, and $G(q) \in \mathbb{R}^{13}$ is the gravity vector. $K_{\text{spring}}\,q \in \mathbb{R}^{13}$ and $K_{\text{damper}}\,\dot{q} \in \mathbb{R}^{13}$ denote the force terms associated with the series elastic elements.

C. Single support phase with yaw friction about the stance leg end

The objective of this section is to consider the yaw friction about the stance leg end during the right stance phase. An analogous analysis can be presented during the left stance phase. Let $\omega^z_{f\mathrm{R}} \in \mathbb{R}$ be the angular velocity corresponding to the yaw motion of the right foot with respect to the world frame. It is assumed that the yaw friction about the stance leg end can be expressed as the viscous model

$$f_{\text{friction}}(q, \dot{q}) := \gamma_{\text{friction}}\,\omega^z_{f\mathrm{R}}(q, \dot{q}) := \gamma_{\text{friction}}\,E^z_{f\mathrm{R}}(q)\,\dot{q}, \tag{3}$$

where $\gamma_{\text{friction}} > 0$ is the viscous friction coefficient and

$$E^z_{f\mathrm{R}}(q) := \frac{\partial \omega^z_{f\mathrm{R}}}{\partial \dot{q}} \in \mathbb{R}^{1\times13}. \tag{4}$$

(Uncertainty in the friction coefficient is addressed in the control design.) Considering the principle of virtual work, the vector $H(q, \dot{q})$ in (2) together with the friction at the stance leg end is revised as follows[2]

$$\begin{aligned} H(q, \dot{q}) := {} & C(q, \dot{q})\,\dot{q} + G(q) + K_{\text{spring}}\,q + K_{\text{damper}}\,\dot{q} \\ & + \gamma_{\text{friction}}\,E^{z'}_{f\mathrm{R}}(q)\,E^z_{f\mathrm{R}}(q)\,\dot{q}. \end{aligned} \tag{5}$$

Finally, the evolution of the mechanical system during the right and left stance phases can be represented by $\dot{x} = f_{\mathrm{R}}(x) + g_{\mathrm{R}}(x)\,u$ and $\dot{x} = f_{\mathrm{L}}(x) + g_{\mathrm{L}}(x)\,u$.

D. Impact model

This section addresses the impact maps during the right-to-left and left-to-right transitions. It is assumed that the impacts are instantaneous and inelastic. In addition, we assume that the impact preserves the yaw orientation of the swing leg end. To develop the impact map during the left-to-right transition, we make use of the *extended model*, in which the generalized coordinates vector of the mechanical system is augmented by adding the Cartesian coordinates of the stance leg end. An analogous approach can be presented during the right-to-left transition. Following the approach of references [30] and [28], (1) conservation of momentum during the impact together with (2) the swing leg neither slipping nor rebounding, and (3) preserving the swing foot orientation results in

$$\begin{bmatrix} \dot{q}^+_e \\ \delta F_{\mathrm{R}} \end{bmatrix} = \begin{bmatrix} D_e(q^-_e) & -E'_{f\mathrm{R},e}(q^-_e) \\ E_{f\mathrm{R},e}(q^-_e) & 0_{4\times4} \end{bmatrix}^{-1} \begin{bmatrix} D_e(q^-_e)\,\dot{q}^-_e \\ 0_4 \end{bmatrix}. \tag{6}$$

In (6), $q_e := (q', p'_{f\mathrm{L}})' \in \mathcal{Q} \times \mathbb{R}^3 =: \mathcal{Q}_e$ and $\dot{q}_e := (\dot{q}', \dot{p}'_{f\mathrm{L}})' \in \mathbb{R}^{16}$ denote the extended generalized coordinates and velocities, respectively. $\delta F_{\mathrm{R}} \in \mathbb{R}^4$ is also the Lagrange multipliers vector referred to as the *impulsive forces and moment at the right leg end*. The subscript "e" represents the quantities related to the extended model. The superscripts "$-$" and "$+$" denote the quantities just before and after the impact. Furthermore, $D_e \in \mathbb{R}^{16\times16}$ is the extended mass-inertia matrix and $E_{f\mathrm{R},e} \in \mathbb{R}^{4\times16}$ is the extended Jacobian matrix at the swing (right) leg end as follows

$$E_{f\mathrm{R},e}(q_e) := \begin{bmatrix} \frac{\partial p_{f\mathrm{R}}}{\partial q_e}(q_e) \\ \frac{\partial \omega^z_{f\mathrm{R}}}{\partial \dot{q}_e}(q_e) \end{bmatrix}. \tag{7}$$

We note that the angular velocity $\omega^z_{f\mathrm{R}}$ is linear with respect to $\dot{q}_e$. Thus, according to [8], [31] the position and orientation of the foot being fixed during impact can be expressed as

[2]According to the principle of virtual work, the friction term appears as $E^{z'}_{f\mathrm{R}}(q)\,f_{\text{friction}}(q, \dot{q}) = \gamma_{\text{friction}}\,E^{z'}_{f\mathrm{R}}(q)\,E^z_{f\mathrm{R}}(q)\,\dot{q}$ in the dynamical equation.

$E_{fR,e}(q_e)\,\dot{q}_e^+ = 0_4$. Finally, the right-to-left and left-to-right impact maps can be expressed as $\Delta_{R\to L} : \mathcal{S}_{R\to L} \to T\mathcal{Q}$ and $\Delta_{L\to R} : \mathcal{S}_{L\to R} \to T\mathcal{Q}$.

E. Hybrid model

The overall model of 3D walking can be expressed as a hybrid system consisting of two continuous phases and two discrete transitions between them as follows

$$\Sigma_R : \begin{cases} \dot{x} = f_R(x) + g_R(x)\,u, & x^- \notin \mathcal{S}_{R\to L} \\ x^+ = \Delta_{R\to L}(x^-), & x^- \in \mathcal{S}_{R\to L} \end{cases}$$
$$\Sigma_L : \begin{cases} \dot{x} = f_L(x) + g_L(x)\,u, & x^- \notin \mathcal{S}_{L\to R} \\ x^+ = \Delta_{L\to R}(x^-), & x^- \in \mathcal{S}_{L\to R}. \end{cases} \tag{8}$$

III. Symmetry between the Right and Left Stance Phases

The objective of this section is to present the symmetry between the right and left stance phases. Let $\mathcal{O} \subset \mathcal{X}$ be a symmetric periodic orbit corresponding to ATRIAS walking along the y-axis of the world frame, the direction of forward walking as indicated in Fig. 1. Then, $\mathcal{O}$ can be decomposed as $\mathcal{O} = \mathcal{O}_R \cup \mathcal{O}_L$, in which $\mathcal{O}_R$ and $\mathcal{O}_L$ are the orbits during the right and left stance phases, respectively. In addition, assume that T^* is the common elapsed time to complete a step on $\mathcal{O}_R$ and $\mathcal{O}_L$. The gait being symmetric along the y-axis of the world frame means that on $\mathcal{O}$

$$q(t + T^*) = \mathbf{S}\,q(t), \quad \forall\, t, \tag{9}$$

in which $\mathbf{S} := \text{block diag}\{\mathbf{S}_1, \mathbf{S}_2\} \in \mathbb{R}^{13\times 13}$ is the *symmetry matrix*. In addition, $\mathbf{S}_1 := \text{diag}\{-1, -1, 1\}$ considers the symmetry for the yaw, roll and pitch angles of the torso link during consecutive steps on $\mathcal{O}$ and $\mathbf{S}_2 \in \mathbb{R}^{10\times 10}$ is a matrix that swaps the role of $\{q_{1R}, q_{2R}, q_{gr1R}, q_{gr2R}, q_{3R}\}$ (relative right variables) by $\{q_{1L}, q_{2L}, q_{gr1L}, q_{gr2L}, q_{3L}\}$ (relative left variables) and vice versa. For later purposes, we remark that $\mathbf{S}\,\mathbf{S} = I_{13\times 13}$.

Theorem 1 (Symmetry in the Hybrid Model): Let D_R, D_L, C_R, C_L, G_R, G_L, H_R, and H_L denote the dynamic terms during the right and left stance phases[3]. Moreover, define

$$\bar{\mathbf{S}} := \text{block diag}\{\mathbf{S}, \mathbf{S}\} \in \mathbb{R}^{26\times 26} \tag{10}$$

as the full-state symmetry matrix. Assume that the model of ATRIAS is symmetric with respect to the yz-plane of the torso frame. Then, the following statements are true.

1) For every $(q', \dot{q}')' \in T\mathcal{Q}$, $D_L(q) = \mathbf{S}'\,D_R(\mathbf{S}\,q)\,\mathbf{S}$, $C_L(q, \dot{q}) = \mathbf{S}'\,C_R(\mathbf{S}\,q, \mathbf{S}\,\dot{q})\,\mathbf{S}$, $G_L(q) = \mathbf{S}'\,G_R(\mathbf{S}\,q)$, and $H_L(q, \dot{q}) = \mathbf{S}'\,H_R(\mathbf{S}\,q, \mathbf{S}\,\dot{q})$.
2) For every $x^- \in \mathcal{S}_{L\to R}$,

$$\Delta_{L\to R}(q^-, \dot{q}^-) = \bar{\mathbf{S}}\,\Delta_{R\to L}(\mathbf{S}\,q^-, \mathbf{S}\,\dot{q}^-).$$

Proof: See Appendix A. ∎

[3]Since q and u vectors are same for the right and left stance phases, the input matrix B is same during the right and left single support phases.

IV. Hybrid Control Strategy on the Basis of One-Step Event-Based Update Law

In order to asymptotically stabilize periodic gaits for 3D walking by ATRIAS, this section presents a time-invariant hybrid control strategy on the basis of symmetry. The *continuous-time* portion of the hybrid controller employs a general class of time-invariant feedback laws assumed to be piecewise continuously differentiable. Furthermore, they are parameterized by a set of finite-dimensional parameters referred to as the *stabilizing parameters*. It is also assumed that there exists a set of nominal parameters for which the periodic orbit $\mathcal{O}$ is an integral curve of the closed-loop hybrid model. The *discrete-time* portion of the hybrid controller is designed on the basis of left-right symmetry to update the parameters of the feedback laws in a one-step manner.

A. Continuous-time portion of the hybrid control strategy

This section allows for a general class of piecewise-defined and parameterized continuous-time feedback laws for which asymptotic and robust stabilization will be addressed in Sections IV-D and V, respectively. The motivation behind a piecewise-defined feedback law is that we would like to begin attenuating the effects of an external push by updating controller parameters within the step the disturbance occurs. If the parameter update is performed either at the beginning or end of the current step, the controller is effectively postponing action to the step following the disturbance. Such a control policy can be expressed as a feedback law whose parameters are updated when a real-valued function of the state variables, referred to as the *phasing term*, passes a specific threshold value and hence, the feedback laws are piecewise-defined. In particular, before the phasing term reaches the threshold value, the controller employs a set of nominal parameters corresponding to the periodic orbit, whereas when the phasing term reaches the threshold value for stabilization, the parameters are updated. To present the main idea, we assume that the following hypothesis is satisfied for the periodic orbit $\mathcal{O}$.

H1) There are $\mathcal{C}^1$ real-valued functions $\tau_R(q)$ and $\tau_L(q)$, referred to as the *phasing terms*, which are strictly increasing functions of time on $\mathcal{O}_R$ and $\mathcal{O}_L$, respectively. Moreover, for every $q \in \mathcal{Q}$ and $i, j \in \{R, L\}$ with the property $i \neq j$,

$$\tau_i(q) = \tau_j(\mathbf{S}\,q). \tag{11}$$

Hypothesis H1 is not restrictive and it implies the existence of strictly increasing holonomic quantities which are invariant under the $\mathbf{S}$ action during the right and left stance phases of walking. For typical walking motions, $\tau_i(q)$, $i \in \{R, L\}$ can be chosen as the horizontal displacement of the center of mass (COM) in the sagittal plane relative to the stance leg end. For later purposes, we assume that on each phase of the periodic orbit, the phasing term $\tau_i(q), i \in \{R, L\}$ belongs to the set $[\tau_{\min}, \tau_{\max})$, where $\tau_{\min} < \tau_{\max}$. Next, let $\mathcal{B}_R \subset \mathbb{R}^p$ and $\mathcal{B}_L \subset \mathbb{R}^p$ be finite-dimensional parameter spaces, referred to as the *right and left stabilizing parameter spaces*, respectively, for some $p > 0$. For every $i \in \{R, L\}$, define a family of

piecewise-defined and parameterized feedback laws $\Gamma_i : \mathcal{X} \times \mathcal{B}_i \to \mathcal{U}$ by the following policy

$$\Gamma_i(x, \beta_i) := \begin{cases} \text{fcn}_i(x, \beta_i^*), & \tau_i(q) < \tau_{\text{th}} \\ \text{fcn}_i(x, \beta_i), & \tau_i(q) \geq \tau_{\text{th}}, \end{cases} \tag{12}$$

where $\beta_i \in \mathcal{B}_i$ denote the *stabilizing parameters* to be used for $\tau_i(q) \geq \tau_{\text{th}}$. In (12), $\text{fcn}_i : \mathcal{X} \times \mathcal{B}_i \to \mathcal{U}$ for $i \in \{\text{R}, \text{L}\}$ are $\mathcal{C}^1$ functions with respect to (x, β_i) on $\mathcal{X} \times \mathcal{B}_i$. Moreover, $\beta_i^* \in \mathcal{B}_i, i \in \{\text{R}, \text{L}\}$ denotes a set of *nominal stabilizing parameters* which are used for $\tau_i(q) < \tau_{\text{th}}$. $\tau_{\text{th}} \in (\tau_{\min}, \tau_{\max})$ represents a to-be-determined threshold value of τ_i. Next, associated with τ_i and τ_{th}, the event-based control surface during phase i can be defined as follows

$$\mathcal{T}_{\text{th},i} := \{(q', \dot{q}')' \in \mathcal{X} | \, \tau_i(q) = \tau_{\text{th}}\} \tag{13}$$

on which the parameters are updated from the nominal value β_i^* to β_i for stabilization and disturbance rejection. For later purposes, this surface will be taken as the Poincaré section. It is further assumed that the following hypothesis is satisfied.

H2) On the surface $\mathcal{T}_{\text{th},i}$, $i \in \{\text{R}, \text{L}\}$,

$$\text{(i)} \quad \text{fcn}_i(x, \beta_i^*) = \text{fcn}_i(x, \beta_i)$$
$$\text{(ii)} \quad \frac{\partial \text{fcn}_i}{\partial x}(x, \beta_i^*) = \frac{\partial \text{fcn}_i}{\partial x}(x, \beta_i)$$
$$\text{(iii)} \quad \frac{\partial \text{fcn}_i}{\partial \beta_i}(x, \beta_i^*) = 0_{6 \times p},$$

which in turn implies that the feedback law Γ_i is $\mathcal{C}^1$ with respect to (x, β_i) on $\mathcal{X} \times \mathcal{B}_i$.

By employing the parameterized feedback law (12), the closed-loop hybrid model of walking (8) can be expressed as

$$\Sigma_{\text{cl,R},\beta_{\text{R}}} : \begin{cases} \dot{x} = f_{\text{cl,R}}(x, \beta_{\text{R}}), & x^- \notin \mathcal{S}_{\text{R}\to\text{L}} \\ x^+ = \Delta_{\text{R}\to\text{L}}(x^-), & x^- \in \mathcal{S}_{\text{R}\to\text{L}} \end{cases}$$
$$\Sigma_{\text{cl,L},\beta_{\text{L}}} : \begin{cases} \dot{x} = f_{\text{cl,L}}(x, \beta_{\text{L}}), & x^- \notin \mathcal{S}_{\text{L}\to\text{R}} \\ x^+ = \Delta_{\text{L}\to\text{R}}(x^-), & x^- \in \mathcal{S}_{\text{L}\to\text{R}}, \end{cases} \tag{14}$$

in which $f_{\text{cl},i}(x, \beta_i) := f_i(x) + g_i(x)\,\Gamma_i(x, \beta_i)$ for $i \in \{\text{R}, \text{L}\}$. For simplicity, we denote the parameterized hybrid model of (14) by $\mathcal{H}(\Sigma_{\text{cl,R},\beta_{\text{R}}}, \Sigma_{\text{cl,L},\beta_{\text{L}}})$. Throughout this paper, we shall assume that the following hypothesis is met.

H3) Associated with the nominal stabilizing parameters $\beta_i^* \in \mathcal{B}_i$, $i \in \{\text{R}, \text{L}\}$, the periodic orbit $\mathcal{O} = \mathcal{O}_{\text{R}} \cup \mathcal{O}_{\text{L}}$ is an integral curve of the hybrid system $\mathcal{H}(\Sigma_{\text{cl,R},\beta_{\text{R}}^*}, \Sigma_{\text{cl,L},\beta_{\text{L}}^*})$. Moreover, for every $i, j \in \{\text{R}, \text{L}\}$ and $i \neq j$, the orbit $\mathcal{O}_i$ is transversal to the switching manifold $\mathcal{S}_{i\to j}$ and also to the event-based control surface $\mathcal{T}_{\text{th},i}$. In particular, $\{x_i^*\} := \overline{\mathcal{O}}_i \cap \mathcal{S}_{i\to j}$ and $\{x_{\text{th},i}^*\} := \overline{\mathcal{O}}_i \cap \mathcal{T}_{\text{th},i}$ are singletons, where $\overline{\mathcal{O}}_i$ is the set closure of $\mathcal{O}_i$.

The following theorem presents the symmetry between the right and left feedback laws on the periodic orbit $\mathcal{O}$.

Theorem 2 (Symmetry in Continuous-Time Feedback Laws): Assume that the model of ATRIAS is symmetric with respect to the yz-plane of the torso frame and hypotheses H1-H3 are satisfied. Then, the periodic orbit is symmetric in the sense of (9) if and only if for every $(q', \dot{q}')' \in \mathcal{O}_{\text{L}}$,

$$B\,\text{fcn}_{\text{L}}(q, \dot{q}, \beta_{\text{L}}^*) = \mathbf{S}'\,B\,\text{fcn}_{\text{R}}(\mathbf{S}\,q, \mathbf{S}\,\dot{q}, \beta_{\text{R}}^*). \tag{15}$$

Proof: (Necessity Part) Under the symmetry condition of the periodic orbit, for every $(q', \dot{q}')' \in \mathcal{O}_{\text{L}}$, it can be concluded that $((\mathbf{S}\,q)', (\mathbf{S}\,\dot{q})')' \in \mathcal{O}_{\text{R}}$. This together with hypotheses H1 and H3 implies that

$$D_{\text{L}}(q)\,\ddot{q} + H_{\text{L}}(q, \dot{q}) = B\,\text{fcn}_{\text{L}}(q, \dot{q}, \beta_{\text{L}}^*) \tag{16a}$$
$$D_{\text{R}}(\mathbf{S}\,q)\,\mathbf{S}\,\ddot{q} + H_{\text{R}}(\mathbf{S}\,q, \mathbf{S}\,\dot{q}) = B\,\text{fcn}_{\text{R}}(\mathbf{S}\,q, \mathbf{S}\,\dot{q}, \beta_{\text{R}}^*). \tag{16b}$$

Furthermore, from (16a), in view of Part (1) of Theorem 1, it follows that

$$\mathbf{S}'\,D_{\text{R}}(\mathbf{S}\,q)\,\mathbf{S}\,\ddot{q} + \mathbf{S}'\,H_{\text{R}}(\mathbf{S}\,q, \mathbf{S}\,\dot{q}) = B\,\text{fcn}_{\text{L}}(q, \dot{q}, \beta_{\text{L}}^*). \tag{17}$$

Comparing (17) and (16b) yields (15) for every $(q', \dot{q}')' \in \mathcal{O}_{\text{L}}$.

(Sufficiency Part) Equations (16a) and (15) together with Part (1) of Theorem 1 result in (16b). This in combination with uniqueness of solution, rising from hypothesis H2, implies that if $(q(t), \dot{q}(t)), t \geq 0$ is the solution of the left stance phase on $\mathcal{O}_{\text{L}}$, then $(\mathbf{S}\,q(t), \mathbf{S}\,\dot{q}(t)), t \geq 0$ is the corresponding solution on $\mathcal{O}_{\text{R}}$ which completes the proof. ■

B. Two-step Poincaré map

This section presents the parameterized two-step Poincaré return map for the hybrid model (14). According to the construction procedure of the continuous-time feedback laws in Section IV-A, the two-step Poincaré map can be defined on $\mathcal{T}_{\text{th},i}$, $i \in \{\text{R}, \text{L}\}$. We note that $\dim \mathcal{T}_{\text{th},i} = \dim(\mathcal{X}) - 1 = 25$. Without loss of generality, we study the right-to-right Poincaré map for asymptotic and robust stabilization. To achieve this goal, for a given initial condition $x(0)$ and a given stabilizing parameter $\beta_i \in \mathcal{B}_i$, $i \in \{\text{R}, \text{L}\}$, let $\varphi_i(t; x(0), \beta_i)$ denote the unique solution of the parameterized closed-loop differential equation $\dot{x} = f_{\text{cl},i}(x, \beta_i)$ with the initial condition $x(0)$ over the maximal interval of existence[4]. Next, for every $x(0) \in \mathcal{X}$, the flow $\mathcal{F}_i^- : \mathcal{X} \to \mathcal{T}_{\text{th},i}$ is defined as the solution $\varphi_i(t; x(0), \beta_i^*)$, evaluated on $\mathcal{T}_{\text{th},i}$. In particular,

$$\mathcal{F}_i^-(x(0)) := \varphi_i\left(T_i^-(x(0)); x(0), \beta_i^*\right),$$

in which $T_i^-(x(0)) := \inf\{t \geq 0 | \, \varphi_i(t; x(0), \beta_i^*) \in \mathcal{T}_{\text{th},i}\}$ represents the time of the first impact of φ_i with the hypersurface $\mathcal{T}_{\text{th},i}$. In an analogous manner, for every $i \neq j \in \{\text{R}, \text{L}\}$, $x(0) \in \mathcal{T}_{\text{th},i}$ and $\beta_i \in \mathcal{B}_i$, the flow $\mathcal{F}_i^+ : \mathcal{T}_{\text{th},i} \times \mathcal{B}_i \to \mathcal{S}_{i\to j}$ is defined as the solution $\varphi_i(t; x(0), \beta_i)$, evaluated on $\mathcal{S}_{i\to j}$, i.e.,

$$\mathcal{F}_i^+(x(0), \beta_i) := \varphi_i\left(T_i^+(x(0), \beta_i); x(0), \beta_i\right),$$

where $T_i^+(x(0), \beta_i) := \inf\{t \geq 0 | \, \varphi_i(t; x(0), \beta_i) \in \mathcal{S}_{i\to j}\}$ denotes the time of the first impact of φ_i with the switching manifold $\mathcal{S}_{i\to j}$. Now, we are in a position to present the two-step Poincaré map. Let z represent local coordinates for the 25-dimensional hypersurface $\mathcal{T}_{\text{th},i}$. In particular, there exist

[4]Hypothesis H2 implies the uniqueness of the solutions.

projection and lift maps $\pi_{\text{proj},i}$ and $\pi_{\text{lift},i}$, $i \in \{\text{R,L}\}$ such that for every $x \in \mathcal{T}_{\text{th},i}$,

$$z = \pi_{\text{proj},i}(x) \tag{18a}$$
$$x = \pi_{\text{lift},i}(z). \tag{18b}$$

The right-to-right Poincaré map $P_{\text{R}\to\text{R}} : \mathcal{T}_{\text{th,R}} \times \mathcal{B}_{\text{R}} \times \mathcal{B}_{\text{L}} \to \mathcal{T}_{\text{th,R}}$ can then be defined as

$$\begin{aligned} P_{\text{R}\to\text{R}}(z, \beta_{\text{R}}, \beta_{\text{L}}) := \pi_{\text{proj,R}} \circ \mathcal{F}_{\text{R}}^{-} \circ \Delta_{\text{L}\to\text{R}} \\ \circ \mathcal{F}_{\text{L}}^{+} \left(\mathcal{F}_{\text{L}}^{-} \circ \Delta_{\text{R}\to\text{L}} \circ \mathcal{F}_{\text{R}}^{+} \left(\pi_{\text{lift,R}}(z), \beta_{\text{R}} \right), \beta_{\text{L}} \right), \end{aligned} \tag{19}$$

where "$\circ$" denotes the function composition and $\beta_i, i \in \{\text{R}, \text{L}\}$ is employed for $\tau_i(q) \geq \tau_{\text{th},i}$ during phase i. According to the construction procedure of the continuous feedback laws (12) and hypothesis H3, $P_{\text{R}\to\text{R}}(z^*_{\text{R}}, \beta^*_{\text{R}}, \beta^*_{\text{L}}) = z^*_{\text{R}}$, where $z^*_{\text{R}} := \pi_{\text{proj,R}}(x^*_{\text{th,R}})$. For later purposes, let

$$z_{k+2} = P_{\text{R}\to\text{R}}(z_k, \beta_k) \tag{20}$$

represent a discrete-time system defined on the basis of the right-to-right Poincaré map $P_{\text{R}\to\text{R}}$ given in (19). Here, k denotes the step number which is updated on the event-based control surface $\mathcal{T}_{\text{th},i}, i \in \{\text{R,L}\}$. In order to have a compact equation, $\beta_k \in \mathbb{R}^{2p}$ also includes both the right and left stabilizing parameters. β^* is the corresponding set of nominal parameters associated with $\mathcal{O}$. Next, linearization of (20) about $(z^*_{\text{R}}, \beta^*)$ results in

$$\delta z_{k+2} = A_{\text{R}\to\text{R}}\, \delta z_k + B_{\text{R}\to\text{R}}\, \delta\beta_k, \tag{21}$$

where $\delta z_k := z_k - z^*_{\text{R}}$, $\delta\beta_k := \beta_k - \beta^*$, $A_{\text{R}\to\text{R}} \in \mathbb{R}^{25\times 25}$ and $B_{\text{R}\to\text{R}} \in \mathbb{R}^{25\times 2p}$.

C. Symmetry in the Poincaré maps and Jacobian matrices

This section addresses the symmetry among the Poincaré maps and the corresponding Jacobian matrices to present the one step correction law in Section IV-D. From Section IV-B, z is a set of local coordinates for $\mathcal{T}_{\text{th},i}, i \in \{\text{R,L}\}$. By defining $\delta x := x - x^*_{\text{th},i} \in \mathbb{R}^{26}$, $\delta z := z - z^*_i \in \mathbb{R}^{25}$ and $z^*_i := \pi_{\text{proj},i}(x^*_{\text{th},i})$, while considering the projection and lift maps in (18), it can be concluded that

$$\delta x = \frac{\partial \pi_{\text{lift},i}}{\partial z}(z^*_i)\, \delta z \tag{22a}$$
$$\delta z = \frac{\partial \pi_{\text{proj},i}}{\partial x}(x^*_{\text{th},i})\, \delta x \tag{22b}$$
$$\frac{\partial \pi_{\text{proj},i}}{\partial x}(x^*_{\text{th},i})\, \frac{\partial \pi_{\text{lift},i}}{\partial z}(z^*_i) = I_{25\times 25}. \tag{22c}$$

Next, (21) in the extended coordinates δx can be expressed as

$$\delta x_{k+2} = A^e_{\text{R}\to\text{R}}\, \delta x_k + B^e_{\text{R}\to\text{R}}\, \delta\beta_k, \tag{23}$$

in which

$$A^e_{\text{R}\to\text{R}} := \frac{\partial \pi_{\text{lift,R}}}{\partial z}(z^*_{\text{R}})\, A_{\text{R}\to\text{R}}\, \frac{\partial \pi_{\text{proj,R}}}{\partial x}(x^*_{\text{th,R}}) \in \mathbb{R}^{26\times 26} \tag{24a}$$
$$B^e_{\text{R}\to\text{R}} := \frac{\partial \pi_{\text{lift,R}}}{\partial z}(z^*_{\text{R}})\, B_{\text{R}\to\text{R}} \in \mathbb{R}^{26\times 2p} \tag{24b}$$

are the extended Jacobian matrices. In this section, we assume that the following hypothesis is satisfied for the feedback laws of (12).

H4) There exists matrix $\mathbf{S}_\beta \in \mathbb{R}^{p\times p}$ such that $\mathbf{S}_\beta\, \mathbf{S}_\beta = I_{p\times p}$ and for every $x \in \mathcal{X}$ and $\beta_{\text{L}} \in \mathcal{B}_{\text{L}}$,

$$B\, \text{fcn}_{\text{L}}(x, \beta_{\text{L}}) = \mathbf{S}'\, B\, \text{fcn}_{\text{R}}(\bar{\mathbf{S}}\, x, \mathbf{S}_\beta\, \beta_{\text{L}}). \tag{25}$$

It is remarkable that the symmetric condition of the periodic orbit $\mathcal{O}$ together with hypotheses H1-H3 implies (15), which is fulfilled on $\mathcal{O}$. However, hypothesis H4 is a special requirement to be satisfied for all $x \in \mathcal{X}$ and $\beta_{\text{L}} \in \mathcal{B}_{\text{L}}$. In addition, (15) and hypothesis H4 imply that

$$\beta^*_{\text{R}} = \mathbf{S}_\beta\, \beta^*_{\text{L}}, \quad \beta^*_{\text{L}} = \mathbf{S}_\beta\, \beta^*_{\text{R}}. \tag{26}$$

The following theorem obtains the left-to-left and left-to-right Jacobians based on the right-to-right and right-to-left[5] ones.

Theorem 3 (Symmetry in the Jacobian Matrices): Assume that the model of ATRIAS is symmetric with respect to the yz-plane of the torso frame. Suppose further that the periodic orbit $\mathcal{O}$ is symmetric and hypotheses H1-H4 are satisfied. Then,

$$\begin{aligned} &\text{(i)} \quad A^e_{\text{L}\to\text{R}} = \bar{\mathbf{S}}\, A^e_{\text{R}\to\text{L}}\, \bar{\mathbf{S}}, \quad B^e_{\text{L}\to\text{R}} = \bar{\mathbf{S}}\, B^e_{\text{R}\to\text{L}}\, \mathbf{S}_\beta \\ &\text{(ii)} \quad A^e_{\text{L}\to\text{L}} = \bar{\mathbf{S}}\, A^e_{\text{R}\to\text{R}}\, \bar{\mathbf{S}}, \end{aligned} \tag{27}$$

where $\bar{\mathbf{S}}$ was defined in (10).

Proof: The linearization of the extended right-to-left Poincaré map can be given by[6]

$$\delta x_{k+1} = A^e_{\text{R}\to\text{L}}\, \delta x_k + B^e_{\text{R}\to\text{L}}\, \delta\beta_{\text{R},k}, \tag{28}$$

where $\delta\beta_{\text{R},k}$ represents the right components of $\delta\beta$ applied during the k^{th} step. In an analogous manner,

$$\delta x_{k+2} = A^e_{\text{L}\to\text{R}}\, \delta x_{k+1} + B^e_{\text{L}\to\text{R}}\, \delta\beta_{\text{L},k+1}, \tag{29}$$

is the linearization of the extended left-to-right Poincaré map and $\delta\beta_{\text{L},k+1}$ is the corresponding components applied during left stance ($k+1^{th}$ step). Next, (28), (29) and

$$\delta\beta_k = \begin{bmatrix} \delta\beta_{\text{R},k} \\ \delta\beta_{\text{L},k+1} \end{bmatrix},$$

while considering (23), yield $A^e_{\text{R}\to\text{R}} = A^e_{\text{L}\to\text{R}}\, A^e_{\text{R}\to\text{L}}$ and

$$B^e_{\text{R}\to\text{R}} = \begin{bmatrix} A^e_{\text{L}\to\text{R}}\, B^e_{\text{R}\to\text{L}} & B^e_{\text{L}\to\text{R}} \end{bmatrix}.$$

Similar reasoning also results in $A^e_{\text{L}\to\text{L}} = A^e_{\text{R}\to\text{L}}\, A^e_{\text{L}\to\text{R}}$ and

$$B^e_{\text{L}\to\text{L}} = \begin{bmatrix} B^e_{\text{R}\to\text{L}} & A^e_{\text{R}\to\text{L}}\, B^e_{\text{L}\to\text{R}} \end{bmatrix}.$$

Moreover, Part (1) of Theorem 1 together with $\mathbf{S} = \mathbf{S}^{-1}$, $\bar{\mathbf{S}} = \bar{\mathbf{S}}^{-1}$ and hypothesis H4 yields

$$\begin{aligned} f_{\text{L}}(x) &= \begin{bmatrix} \dot{q} \\ -D_{\text{L}}^{-1}(q)\, H_{\text{L}}(q, \dot{q}) \end{bmatrix} \\ &= \begin{bmatrix} \mathbf{S}^{-1}\, \mathbf{S}\, \dot{q} \\ -\mathbf{S}^{-1}\, D_{\text{R}}^{-1}(\mathbf{S}\, q)\, (\mathbf{S}')^{-1}\, \mathbf{S}'\, H_{\text{R}}(\mathbf{S}\, q, \mathbf{S}\, \dot{q}) \end{bmatrix} \\ &= \bar{\mathbf{S}}\, f_{\text{R}}(\bar{\mathbf{S}}\, x) \end{aligned}$$

[5]The right-to-left Poincaré map is defined from $\mathcal{T}_{\text{th,R}}$ during right stance to $\mathcal{T}_{\text{th,L}}$ during left stance. Similar definitions can be presented for the left-to-right as well as the left-to-left Poincaré maps.

[6]According to hypotheses H1-H3 and [6, p. 89], the Poincaré maps are $\mathcal{C}^1$ in an open neighborhood of the periodic orbit $\mathcal{O}$.

and

$$g_{\mathrm{L}}(x)\,\Gamma_{\mathrm{L}}(x,\beta_{\mathrm{L}}) = \begin{bmatrix} 0_{13\times 1} \\ D_{\mathrm{L}}^{-1}(q)\,B\,\Gamma_{\mathrm{L}}(x,\beta_{\mathrm{L}}) \end{bmatrix} = \begin{bmatrix} 0_{13\times 1} \\ \mathbf{S}^{-1}\,D_{\mathrm{R}}^{-1}(\mathbf{S}\,q)\,(\mathbf{S}')^{-1}\,\mathbf{S}'\,B\,\Gamma_{\mathrm{R}}(\bar{\mathbf{S}}\,x,\mathbf{S}_\beta\,\beta_{\mathrm{L}}) \end{bmatrix} = \bar{\mathbf{S}}\,g_{\mathrm{R}}(\bar{\mathbf{S}}\,x)\,\Gamma_{\mathrm{R}}(\bar{\mathbf{S}}\,x,\mathbf{S}_\beta\,\beta_{\mathrm{L}}),$$

which in turn implies that

$$f_{\mathrm{cl,L}}(x,\beta_{\mathrm{L}}) = \bar{\mathbf{S}}\,f_{\mathrm{cl,R}}(\bar{\mathbf{S}}\,x,\mathbf{S}_\beta\,\beta_{\mathrm{L}}). \tag{30}$$

Next, from (11) and (13), it can be concluded that for every $x \in \mathcal{T}_{\mathrm{th,L}}$, $\bar{\mathbf{S}}\,x \in \mathcal{T}_{\mathrm{th,R}}$. An analogous result can also be presented for the switching manifolds $\mathcal{S}_{\mathrm{R}\to\mathrm{L}}$ and $\mathcal{S}_{\mathrm{L}\to\mathrm{R}}$. This in combination with (30) results in $\mathcal{F}_{\mathrm{L}}^{-}(x) = \bar{\mathbf{S}}\,\mathcal{F}_{\mathrm{R}}^{-}(\bar{\mathbf{S}}\,x)$ and $\mathcal{F}_{\mathrm{L}}^{+}(x,\beta_{\mathrm{L}}) = \bar{\mathbf{S}}\,\mathcal{F}_{\mathrm{R}}^{+}(\bar{\mathbf{S}}\,x,\mathbf{S}_\beta\,\beta_{\mathrm{L}})$. The extended right-to-left and left-to-right Poincaré maps can then be expressed as

$$P_{\mathrm{R}\to\mathrm{L}}^{e}(x,\beta_{\mathrm{R}}) := \mathcal{F}_{\mathrm{L}}^{-} \circ \Delta_{\mathrm{R}\to\mathrm{L}} \circ \mathcal{F}_{\mathrm{R}}^{+}(x,\beta_{\mathrm{R}})$$
$$P_{\mathrm{L}\to\mathrm{R}}^{e}(x,\beta_{\mathrm{L}}) := \mathcal{F}_{\mathrm{R}}^{-} \circ \Delta_{\mathrm{L}\to\mathrm{R}} \circ \mathcal{F}_{\mathrm{L}}^{+}(x,\beta_{\mathrm{L}})$$

for which, the following property is fulfilled[7]

$$\begin{aligned} P_{\mathrm{L}\to\mathrm{R}}^{e}(x,\beta_{\mathrm{L}}) &= \mathcal{F}_{\mathrm{R}}^{-} \circ \Delta_{\mathrm{L}\to\mathrm{R}} \circ \mathcal{F}_{\mathrm{L}}^{+}(x,\beta_{\mathrm{L}}) \\ &= \mathcal{F}_{\mathrm{R}}^{-} \circ \Delta_{\mathrm{L}\to\mathrm{R}} \left(\bar{\mathbf{S}}\,\mathcal{F}_{\mathrm{R}}^{+}(\bar{\mathbf{S}}\,x,\mathbf{S}_\beta\,\beta_{\mathrm{L}})\right) \\ &= \mathcal{F}_{\mathrm{R}}^{-} \left(\bar{\mathbf{S}}\,\Delta_{\mathrm{R}\to\mathrm{L}} \circ \mathcal{F}_{\mathrm{R}}^{+}(\bar{\mathbf{S}}\,x,\mathbf{S}_\beta\,\beta_{\mathrm{L}})\right) \\ &= \bar{\mathbf{S}}\,\mathcal{F}_{\mathrm{L}}^{-} \circ \Delta_{\mathrm{R}\to\mathrm{L}} \circ \mathcal{F}_{\mathrm{R}}^{+}(\bar{\mathbf{S}}\,x,\mathbf{S}_\beta\,\beta_{\mathrm{L}}) \\ &= \bar{\mathbf{S}}\,P_{\mathrm{R}\to\mathrm{L}}^{e}(\bar{\mathbf{S}}\,x,\mathbf{S}_\beta\,\beta_{\mathrm{L}}). \end{aligned} \tag{31}$$

Next, according to (31) and (26),

$$\frac{\partial P_{\mathrm{L}\to\mathrm{R}}^{e}}{\partial x}(x_{\mathrm{th,L}}^{*},\beta_{\mathrm{L}}^{*}) = \bar{\mathbf{S}}\,\frac{\partial P_{\mathrm{R}\to\mathrm{L}}^{e}}{\partial x}(x_{\mathrm{th,R}}^{*},\beta_{\mathrm{R}}^{*})\,\bar{\mathbf{S}}$$
$$\frac{\partial P_{\mathrm{L}\to\mathrm{R}}^{e}}{\partial \beta_{\mathrm{L}}}(x_{\mathrm{th,L}}^{*},\beta_{\mathrm{L}}^{*}) = \bar{\mathbf{S}}\,\frac{\partial P_{\mathrm{R}\to\mathrm{L}}^{e}}{\partial \beta_{\mathrm{R}}}(x_{\mathrm{th,R}}^{*},\beta_{\mathrm{R}}^{*})\,\mathbf{S}_\beta.$$

In particular, $A_{\mathrm{L}\to\mathrm{R}}^{e} = \bar{\mathbf{S}}\,A_{\mathrm{R}\to\mathrm{L}}^{e}\,\bar{\mathbf{S}}$, $B_{\mathrm{L}\to\mathrm{R}}^{e} = \bar{\mathbf{S}}\,B_{\mathrm{R}\to\mathrm{L}}^{e}\,\mathbf{S}_\beta$ and

$$A_{\mathrm{R}\to\mathrm{R}}^{e} = A_{\mathrm{L}\to\mathrm{R}}^{e}\,A_{\mathrm{R}\to L}^{e} = \bar{\mathbf{S}}\,A_{\mathrm{R}\to\mathrm{L}}^{e}\,\bar{\mathbf{S}}\,A_{\mathrm{R}\to\mathrm{L}}^{e}$$
$$A_{\mathrm{L}\to\mathrm{L}}^{e} = A_{\mathrm{R}\to\mathrm{L}}^{e}\,A_{\mathrm{L}\to\mathrm{R}}^{e} = A_{\mathrm{R}\to\mathrm{L}}^{e}\,\bar{\mathbf{S}}\,A_{\mathrm{R}\to\mathrm{L}}^{e}\,\bar{\mathbf{S}}$$

which completes the proof. ■

D. Time-invariant one-step event-based controller

The objective of this section is to present a time-invariant and one-step event-based controller based on the symmetry of the Poincaré maps. For this goal, assume that the following hypothesis is satisfied for the projection and lift maps in (18).

H5) There exists matrix $\mathbf{S}_z \in \mathbb{R}^{25\times 25}$ such that $\mathbf{S}_z\,\mathbf{S}_z = I_{25\times 25}$ and

$$\begin{aligned} \pi_{\mathrm{proj,L}}(x) &= \mathbf{S}_z\,\pi_{\mathrm{proj,R}}(\bar{\mathbf{S}}\,x), && \forall x \in \mathcal{T}_{\mathrm{th,R}} \\ \pi_{\mathrm{lift,L}}(z) &= \bar{\mathbf{S}}\,\pi_{\mathrm{lift,R}}(\mathbf{S}_z\,z), && \forall z \in \mathbb{R}^{25}. \end{aligned} \tag{32}$$

We remark that $\bar{\mathbf{S}} \in \mathbb{R}^{26\times 26}$ is the full-state symmetry matrix whereas $\mathbf{S}_z \in \mathbb{R}^{25\times 25}$ represents the symmetry matrix for the z (local) coordinates on the Poincaré sections $\mathcal{T}_{\mathrm{th},i}$, $i \in \{\mathrm{R},\mathrm{L}\}$. Furthermore, hypothesis H5 for a symmetric periodic orbit $\mathcal{O}$ immediately implies that $z_{\mathrm{L}}^{*} = \mathbf{S}_z\,z_{\mathrm{R}}^{*}$ and $z_{\mathrm{R}}^{*} = \mathbf{S}_z\,z_{\mathrm{L}}^{*}$.

[7]We remark that $\bar{\mathbf{S}}\,\bar{\mathbf{S}} = I_{26\times 26}$.

Theorem 4 (One-Step Event-Based Law): Assume that the model of ATRIAS is symmetric with respect to the yz-plane of the torso frame. Moreover, suppose that the periodic orbit $\mathcal{O}$ is symmetric and hypotheses H1-H5 are satisfied. Then,

$$P_{\mathrm{R}\to\mathrm{R}}(z,\beta_{\mathrm{R}},\beta_{\mathrm{L}}) = \mathbf{S}_z\,P_{\mathrm{R}\to\mathrm{L}}\left(\mathbf{S}_z\,P_{\mathrm{R}\to\mathrm{L}}(z,\beta_{\mathrm{R}}),\mathbf{S}_\beta\,\beta_{\mathrm{L}}\right). \tag{33}$$

In addition, let $\kappa_{\mathrm{R}}(\bar{z})$ be a continuous (resp. continuously differentiable) function such that (i) $\kappa_{\mathrm{R}}(z_{\mathrm{R}}^{*}) = \beta_{\mathrm{R}}^{*}$ and (ii) z_{R}^{*} is asymptotically (resp. exponentially) stable for the following one-step map[8]

$$\bar{z}_{k+1} = \mathcal{F}_{\text{one-step}}(\bar{z}_k) := \mathbf{S}_z\,P_{\mathrm{R}\to\mathrm{L}}(\bar{z}_k,\kappa_{\mathrm{R}}(\bar{z}_k)). \tag{34}$$

Then, z_{R}^{*} is asymptotically (resp. exponentially) stable for (20), in which

$$\beta_k = \begin{bmatrix} \kappa_{\mathrm{R}}(z_k) \\ \mathbf{S}_\beta\,\kappa_{\mathrm{R}}\left(\mathbf{S}_z\,P_{\mathrm{R}\to\mathrm{L}}(z_k,\kappa_{\mathrm{R}}(z_k))\right) \end{bmatrix}. \tag{35}$$

Proof: Let

$$P_{\mathrm{R}\to\mathrm{L}}(z,\beta_{\mathrm{R}}) := \pi_{\mathrm{proj,L}} \circ P_{\mathrm{R}\to\mathrm{L}}^{e}(\pi_{\mathrm{lift,R}}(z),\beta_{\mathrm{R}})$$
$$P_{\mathrm{L}\to\mathrm{R}}(z,\beta_{\mathrm{L}}) := \pi_{\mathrm{proj,R}} \circ P_{\mathrm{L}\to\mathrm{R}}^{e}(\pi_{\mathrm{lift,L}}(z),\beta_{\mathrm{L}}).$$

From hypotheses H1-H5 and (31), it can be concluded that

$$\begin{aligned} P_{\mathrm{L}\to\mathrm{R}}(z,\beta_{\mathrm{L}}) &= \pi_{\mathrm{proj,R}} \circ P_{\mathrm{L}\to\mathrm{R}}^{e}(\pi_{\mathrm{lift,L}}(z),\beta_{\mathrm{L}}) \\ &= \pi_{\mathrm{proj,R}} \left(\bar{\mathbf{S}}\,P_{\mathrm{R}\to\mathrm{L}}^{e}(\bar{\mathbf{S}}\,\pi_{\mathrm{lift,L}}(z),\mathbf{S}_\beta\,\beta_{\mathrm{L}})\right) \\ &= \pi_{\mathrm{proj,R}} \left(\bar{\mathbf{S}}\,P_{\mathrm{R}\to\mathrm{L}}^{e}(\pi_{\mathrm{lift,R}}(\mathbf{S}_z\,z),\mathbf{S}_\beta\,\beta_{\mathrm{L}})\right) \\ &= \mathbf{S}_z\,\pi_{\mathrm{proj,L}} \circ P_{\mathrm{R}\to\mathrm{L}}^{e}(\pi_{\mathrm{lift,R}}(\mathbf{S}_z\,z),\mathbf{S}_\beta\,\beta_{\mathrm{L}}) \\ &= \mathbf{S}_z\,P_{\mathrm{R}\to\mathrm{L}}(\mathbf{S}_z\,z,\mathbf{S}_\beta\,\beta_{\mathrm{L}}). \end{aligned} \tag{36}$$

This latter equation together with $P_{\mathrm{R}\to\mathrm{R}} := P_{\mathrm{L}\to\mathrm{R}} \circ P_{\mathrm{R}\to\mathrm{L}}$ implies (33). Next, using $\mathbf{S}_\beta\,\mathbf{S}_\beta = I_{p\times p}$ and (35), the evolution of the right-to-right discrete system in (20) can be expressed as

$$\bar{z}_{k+2} = \mathcal{F}_{\text{one-step}} \circ \mathcal{F}_{\text{one-step}}(\bar{z}_k). \tag{37}$$

Standard converse Lyapunov theorems imply the existence of a continuous function $V_{\text{one-step}} : \mathcal{N}_{\text{one-step}} \to \mathbb{R}_{\geq 0}$ such that $V_{\text{one-step}}(z_{\mathrm{R}}^{*}) = 0$, $V_{\text{one-step}}(\bar{z}) > 0$ and $V_{\text{one-step}}\left(\mathcal{F}_{\text{one-step}}(\bar{z})\right) - V_{\text{one-step}}(\bar{z}) < 0$ for all $\bar{z} \in \mathcal{N}_{\text{one-step}} \setminus \{z_{\mathrm{R}}^{*}\}$, where $\mathcal{N}_{\text{one-step}} \subset \mathbb{R}^{25}$ is an open neighborhood of z_{R}^{*}. Since $\mathcal{F}_{\text{one-step}}(z_{\mathrm{R}}^{*}) = z_{\mathrm{R}}^{*}$ and $\mathcal{F}_{\text{one-step}}(.)$ is continuous, $\mathcal{N}_{\text{one-step}}$ can be chosen such that $\mathcal{F}_{\text{one-step}}(\bar{z}) \in \mathcal{N}_{\text{one-step}}$ for all $\bar{z} \in \mathcal{N}_{\text{one-step}}$. Consequently,

$$\begin{aligned} &V_{\text{one-step}}\left(\mathcal{F}_{\text{one-step}} \circ \mathcal{F}_{\text{one-step}}(\bar{z})\right) - V_{\text{one-step}}(\bar{z}) \\ &\quad = V_{\text{one-step}}\left(\mathcal{F}_{\text{one-step}} \circ \mathcal{F}_{\text{one-step}}(\bar{z})\right) - V_{\text{one-step}}\left(\mathcal{F}_{\text{one-step}}(\bar{z})\right) \\ &\quad + V_{\text{one-step}}\left(\mathcal{F}_{\text{one-step}}(\bar{z})\right) - V_{\text{one-step}}(\bar{z}) \\ &\quad < 0, \qquad \forall \bar{z} \in \mathcal{N}_{\text{one-step}} \setminus \{z_{\mathrm{R}}^{*}\}. \end{aligned} \tag{38}$$

Thus, $V_{\text{one-step}}$ is a Lyapunov function for (37) which in turn completes the proof of asymptotic stability. For exponential stability, according to the converse Lyapunov theorem, there are constants $c_1, c_2, c_3 > 0$ such that $c_1\|\bar{z} - z_{\mathrm{R}}^{*}\|^2 \leq V_{\text{one-step}}(\bar{z}) \leq c_2\|\bar{z} - z_{\mathrm{R}}^{*}\|^2$ and $V_{\text{one-step}}\left(\mathcal{F}_{\text{one-step}}(\bar{z})\right) -$

[8]In our notation, $\bar{z}_k := z_k$ during the right stance phase and $\bar{z}_k := \mathbf{S}_z\,z_k$ during the left stance phase.

$V_{\text{one-step}}(\bar{z}) \leq -c_3\|\bar{z} - z_{\text{R}}^*\|^2$ for all $\bar{z} \in \mathcal{N}_{\text{one-step}}$. Next, similar to (38),

$$\begin{aligned} V_{\text{one-step}}&\left(\mathcal{F}_{\text{one-step}} \circ \mathcal{F}_{\text{one-step}}(\bar{z})\right) - V_{\text{one-step}}(\bar{z}) \\ &\leq -c_3\|\bar{z} - z_{\text{R}}^*\|^2 - c_3\|\mathcal{F}_{\text{one-step}}(\bar{z}) - z_{\text{R}}^*\|^2 \\ &\leq -c_3\|\bar{z} - z_{\text{R}}^*\|^2 \qquad \forall \bar{z} \in \mathcal{N}_{\text{one-step}} \end{aligned}$$

which yields exponential stability. ∎

Remark 1 (Application of the One-Step Event-Based Law): Theorem 4 presents the right-to-right Poincaré return map in terms of the one-step map. Furthermore, assume that z_k and z_{k+1} represent the corresponding coordinates on the Poincaré sections during the right (i.e., k^{th}) and left (i.e., $k+1^{st}$) steps, respectively. According to Theorem 4, the event-based laws $\beta_{\text{R}} = \kappa_{\text{R}}(z_k)$ and $\beta_{\text{L}} = \mathbf{S}_\beta\, \kappa_{\text{R}}(\mathbf{S}_z\, z_{k+1})$ asymptotically (exponentially) stabilize the periodic orbit $\mathcal{O}$ for the closed-loop system[9].

V. Robust One-Step Event-Based Control Action

In order to robustly stabilize periodic orbits for 3D walking against numerical and parametric uncertainties as well as external disturbances acting on the robot, this section presents a one-step correction law consisting of two loops. The first loop, referred to as the *robust stabilizer*, introduces an LMI-based time-invariant update law for the one-step map (34) that is designed to be robust against numerical and parametric uncertainties. The objective of the second loop of the discrete action is to increase the basin of attraction as well as the robustness of the closed-loop system against parametric uncertainty and also to reject external disturbances acting on the robot.

A. Robust stabilization

To robustly and asymptotically stabilize the periodic orbit $\mathcal{O}$ against polytopic uncertainties arising from numerical approximation of the Jacobian matrices for the corresponding one-step map, this section presents a discrete and static update law, based on LMIs, for the stabilizing parameters of the continuous-time feedback laws (12). There is no closed-form expression for the 25-dimensional Poincaré return map and consequently, to design event-based update laws, we make use of Jacobian linearization of the Poincaré map. Moreover, the Jacobians are obtained using numerical differentiation, specifically, two-point symmetric differences given by

$$\begin{aligned} &\frac{\partial P_{\text{R}\to\text{L}}}{\partial z_i}(z_{\text{R}}^*, \beta_{\text{R}}^*) = \\ &\qquad \frac{1}{2\varepsilon}\Big(P_{\text{R}\to\text{L}}(z_{\text{R}}^* + \Delta z_i, \beta_{\text{R}}^*) - P_{\text{R}\to\text{L}}(z_{\text{R}}^* - \Delta z_i, \beta_{\text{R}}^*)\Big) \\ &\frac{\partial P_{\text{R}\to\text{L}}}{\partial \beta_i}(z_{\text{R}}^*, \beta_{\text{R}}^*) = \\ &\qquad \frac{1}{2\varepsilon}\Big(P_{\text{R}\to\text{L}}(z_{\text{R}}^*, \beta_{\text{R}}^* + \Delta\beta_i) - P_{\text{R}\to\text{L}}(z_{\text{R}}^*, \beta_{\text{R}}^* - \Delta\beta_i)\Big) \end{aligned}$$

where $\Delta z_i := \varepsilon\, e_i$, $\Delta\beta_i := \varepsilon\, e_i$, ε is the perturbation value and e_i is the standard unit vector in the i-th direction.

[9]We remark that $z_{k+1} = P_{\text{R}\to\text{L}}(z_k, \kappa_{\text{R}}(z_k))$.

In theory, one takes $\varepsilon > 0$ sufficiently small when approximating the derivatives. In practice, selecting ε is not obvious because the dynamic model has multiple scales, due to the heavy body, light leg links, and stiff springs. In other words, the correct perturbation value to calculate the Jacobian matrices based on numerical differentiation algorithms is unknown. This can be formulated as uncertainty in the Jacobian matrices or the Poincaré maps, and it complicates the design of the stabilizing one-step event-based controller in Theorem 4.

The way we handle this uncertainty is to make sure that our event-based control law is insensitive to the value chosen for $\varepsilon > 0$. To achieve this insensitivity, we formally treat the Jacobian linearization as belonging to a family of linearized models and apply robust control theory. In particular, we use a family of perturbation values $\varepsilon_i > 0$ to generate a family of linear models, each rising from different ε values in the set $\mathcal{E} := \{\varepsilon_1, \varepsilon_2, \cdots\}$. In this regard, we present an LMI-based robust control methodology for the one-step map (34). In the proposed approach, let $(A_{\text{LS}}, B_{\text{LS}})$ denote the least square approximation of $(A_{\text{R}\to\text{L}}, B_{\text{R}\to\text{L}})$ over the feasible set of perturbations $\mathcal{E}$. Moreover, $(A_{\text{TPD}}(\varepsilon), B_{\text{TPD}}(\varepsilon))$ represents the two-point symmetric difference estimation of $(A_{\text{R}\to\text{L}}, B_{\text{R}\to\text{L}})$ obtained with the perturbation value $\varepsilon \in \mathcal{E}$. Next, define the convex sets

$$\begin{aligned} \mathbf{A}_{\text{R}\to\text{L}} &:= \text{conv}\{A_{\text{LS}}, A_{\text{TPD}}(\varepsilon) |\, \varepsilon \in \mathcal{E}\} \\ \mathbf{B}_{\text{R}\to\text{L}} &:= \text{conv}\{B_{\text{LS}}, B_{\text{TPD}}(\varepsilon) |\, \varepsilon \in \mathcal{E}\}. \end{aligned} \tag{39}$$

For simplicity, let $A_{\text{R}\to\text{L},m}$ and $B_{\text{R}\to\text{L},n}$ for $m = 1, \cdots, n_{\mathcal{A}}$ and $n = 1, \cdots, n_{\mathcal{B}}$ denote the corresponding vertices of the sets $\mathbf{A}_{\text{R}\to\text{L}}$ and $\mathbf{B}_{\text{R}\to\text{L}}$, respectively. We will suppose that *unknown* Jacobian matrices $A_{\text{R}\to\text{L}}$ and $B_{\text{R}\to\text{L}}$ belong to the sets $\mathbf{A}_{\text{R}\to\text{L}}$ and $\mathbf{B}_{\text{R}\to\text{L}}$. The following theorem presents an LMI-based gain K_{R} which stabilizes z_{R}^* for (34).

Theorem 5 (LMI Stabilization of the Periodic Orbit $\mathcal{O}$): Assume that hypotheses H1-H5 are satisfied and $A_{\text{R}\to\text{L}} \in \mathbf{A}_{\text{R}\to\text{L}}$ and $B_{\text{R}\to\text{L}} \in \mathbf{B}_{\text{R}\to\text{L}}$. Then, the following statements are true.

1) *(Stabilization with known Lyapunov function)* If there exist $Y = Y'$ and Z such that the following set of LMIs

$$\begin{bmatrix} -Y & \mathbf{S}_z\, A_{\text{R}\to\text{L},m}\, Y + \mathbf{S}_z\, B_{\text{R}\to\text{L},n}\, Z \\ \star & -Y \end{bmatrix} < 0 \tag{40}$$

for $m = 1, \cdots, n_{\mathcal{A}}$, $n = 1, \cdots, n_{\mathcal{B}}$ is feasible, then the periodic orbit $\mathcal{O}$ is exponentially stable for the closed-loop system, in which

$$\kappa_{\text{R}}(\bar{z}) := \beta_{\text{R}}^* - K_{\text{R}}\,(\bar{z} - z_{\text{R}}^*) \tag{41}$$

in Theorem 4 and $K_{\text{R}} := -Z\, Y^{-1}$.

2) *(Stabilization with unknown Lyapunov function)* If there exist matrices $T_{mn} = T'_{mn}$ for $m = 1, \cdots, n_{\mathcal{A}}$, $n = 1, \cdots, n_{\mathcal{B}}$, and L and J such that the following set of LMIs

$$\begin{bmatrix} T_{mn} & \mathbf{S}_z\, A_{\text{R}\to\text{L},m}\, L + \mathbf{S}_z\, B_{\text{R}\to\text{L},n}\, J \\ \star & L + L' - T_{mn} \end{bmatrix} > 0 \tag{42}$$

is feasible, then the periodic orbit $\mathcal{O}$ is exponentially stable for the closed-loop system, in which $\kappa_{\text{R}}(\bar{z})$ is given in (41) and $K_{\text{R}} := -J\, L^{-1}$.

Proof: Following hypotheses H1-H3, the Jacobian matrices $A_{\mathrm{R}\to\mathrm{L}}$ and $B_{\mathrm{R}\to\mathrm{L}}$ are well-defined. Moreover, hypothesis H3 and the construction procedure of the feedback laws imply the existence of an open neighborhood $\mathcal{N}$ of $\mathcal{O}$, such that in $\mathcal{N}\setminus\mathcal{O}$, the feedback law $\mathrm{fcn}_{\mathrm{R}}(x,\beta_{\mathrm{R}}^*)$ switches to $\mathrm{fcn}_{\mathrm{R}}(x,\beta_{\mathrm{R}})$ when trajectories cross the Poincaré section $\mathcal{T}_{\text{th,R}}$ which is a necessary condition for $B_{\mathrm{R}\to\mathrm{L}}\neq 0_{25\times p}$.

Part (1): For a given $(A_{\mathrm{R}\to\mathrm{L}},B_{\mathrm{R}\to\mathrm{L}})\in\mathbf{A}_{\mathrm{R}\to\mathrm{L}}\times\mathbf{B}_{\mathrm{R}\to\mathrm{L}}$, there exist $a_m\geq 0$, $m=1,\cdots,n_{\mathcal{A}}$ and $b_n\geq 0$, $n=1,\cdots,n_{\mathcal{B}}$ such that $A_{\mathrm{R}\to\mathrm{L}}=\sum_{m=1}^{n_{\mathcal{A}}}a_m\,A_{\mathrm{R}\to\mathrm{L},m}$ and $B_{\mathrm{R}\to\mathrm{L}}=\sum_{n=1}^{n_{\mathcal{B}}}b_n\,B_{\mathrm{R}\to\mathrm{L},n}$. Moreover, $\sum_{m=1}^{n_{\mathcal{A}}}a_m=\sum_{n=1}^{n_{\mathcal{B}}}b_n=1$. Next,

$$\sum_{m=1}^{n_{\mathcal{A}}}\sum_{n=1}^{n_{\mathcal{B}}}a_m\,b_n\begin{bmatrix}-Y & \mathbf{S}_z\,A_{\mathrm{R}\to\mathrm{L},m}\,Y+\mathbf{S}_z\,B_{\mathrm{R}\to\mathrm{L},n}\,Z\\ \star & -Y\end{bmatrix}=\begin{bmatrix}-Y & \mathbf{S}_z\,A_{\mathrm{R}\to\mathrm{L}}\,Y+\mathbf{S}_z\,B_{\mathrm{R}\to\mathrm{L}}\,Z\\ \star & -Y\end{bmatrix}<0 \tag{43}$$

Using Schur's Lemma, the LMI problem (43) is equivalent to (i) $-Y<0$ and (ii)

$$-Y-(Y\,A'_{\mathrm{R}\to\mathrm{L}}\,\mathbf{S}'_z+Z'\,B'_{\mathrm{R}\to\mathrm{L}}\,\mathbf{S}'_z)\,(-Y)^{-1}\times(\mathbf{S}_z\,A_{\mathrm{R}\to\mathrm{L}}\,Y+\mathbf{S}_z\,B_{\mathrm{R}\to\mathrm{L}}\,Z)<0. \tag{44}$$

Considering $K_{\mathrm{R}}=-ZY^{-1}$, it can be concluded that $V_{\text{one-step}}(\delta\bar{z}):=\delta\bar{z}'\,Y^{-1}\,\delta\bar{z}$ is a Lyapunov function for (34). Finally, applying Theorem 4 and Theorem 4.7 of [6] completes the proof.

Part (2): According to Theorem 3 of [32], if LMIs are feasible, then for every $A_{\mathrm{R}\to\mathrm{L}}\in\mathbf{A}_{\mathrm{R}\to\mathrm{L}}$ and $B_{\mathrm{R}\to\mathrm{L}}\in\mathbf{B}_{\mathrm{R}\to\mathrm{L}}$, $|\mathrm{eig}(\mathbf{S}_z\,A_{\mathrm{R}\to\mathrm{L}}-\mathbf{S}_z\,B_{\mathrm{R}\to\mathrm{L}}\,K_{\mathrm{R}})|<1$ which in turn implies that the z_{R}^* is robustly and exponentially stable for (34) against polytopic uncertainties. Moreover, $V_{\text{one-step}}(\delta\bar{z}):=\delta\bar{z}'\,T\,\delta\bar{z}$ is the corresponding Lyapunov function, in which $T:=\sum_{m=1}^{n_{\mathcal{A}}}\sum_{n=1}^{n_{\mathcal{B}}}a_m\,b_n\,T_{mn}$. This in combination with Theorem 4 and Theorem 4.7 of [6] completes the proof. ∎

Remark 2: Theorem 5 presents two approaches to design the robust and stabilizing one-step event-based law. In the LMI problem of (40), the corresponding Lyapunov function $V_{\text{one-step}}(\delta\bar{z})=\delta\bar{z}'\,Y^{-1}\,\delta\bar{z}$ is known and common for all $(A_{\mathrm{R}\to\mathrm{L}},B_{\mathrm{R}\to\mathrm{L}})\in\mathbf{A}_{\mathrm{R}\to\mathrm{L}}\times\mathbf{B}_{\mathrm{R}\to\mathrm{L}}$, whereas in the LMI problem (42), the Lyapunov function $V_{\text{one-step}}(\delta\bar{z}):=\delta\bar{z}'\,T\,\delta\bar{z}=\sum_{m=1}^{n_{\mathcal{A}}}\sum_{n=1}^{n_{\mathcal{B}}}a_m\,b_n\,V_{mn}(\delta\bar{z})$ depends[10] on $(A_{\mathrm{R}\to\mathrm{L}},B_{\mathrm{R}\to\mathrm{L}})\in\mathbf{A}_{\mathrm{R}\to\mathrm{L}}\times\mathbf{B}_{\mathrm{R}\to\mathrm{L}}$, where $V_{mn}(\delta\bar{z})=\delta\bar{z}'\,T_{mn}\,\delta\bar{z}$ is the corresponding Lyapunov function for the vertex $(A_{\mathrm{R}\to\mathrm{L},m},B_{\mathrm{R}\to\mathrm{L},n})$.

Remark 3: Analogous to Proposition 1 of [28], if (i) the continuous-time feedback law (12) does not depend on the yaw angle and (ii) the column of K_{R} associated with the yaw angle is set to zero in the static update law (41), then the periodic orbit $\mathcal{O}$ is invariant under the group of rotations about the z-axis denoted by $\mathbb{G}$. In this case, the periodic orbit is asymptotically stable "modulo $\mathbb{G}$". This is important because ideally the controller should not be affected by which direction the robot is walking on a flat surface.

[10]Since $a_m,m=1,\cdots,n_{\mathcal{A}}$ and $b_n,n=1,\cdots,n_{\mathcal{B}}$ are unknown, the Lypaunov function is unknown.

B. Robust optimal controller

The objective of this section is to improve the static update law of (41) to reject external disturbances acting on the robot. To achieve this goal, an auxiliary term w_k is introduced to $\kappa_{\mathrm{R}}(\bar{z})$, i.e.,

$$\kappa_{\mathrm{R}}(\bar{z}_k)=\beta_{\mathrm{R}}^*-K_{\mathrm{R}}\,(\bar{z}_k-z_{\mathrm{R}}^*)+w_k. \tag{45}$$

Next, assume that an external force acts on the robot during the right stance phase. Then, the evolution of $\delta\bar{z}_k$ according to the linearized one-step map (34) can be expressed as

$$\delta\bar{z}_{k+1}=A_{\text{one-step,cl}}\,\delta\bar{z}_k+B_{\text{one-step}}\,w_k+F_{\text{one-step}}\,d_k, \tag{46}$$

where $A_{\text{one-step,cl}}:=\mathbf{S}_z\,A_{\mathrm{R}\to\mathrm{L}}-\mathbf{S}_z\,B_{\mathrm{R}\to\mathrm{L}}\,K_{\mathrm{R}}$ and $B_{\text{one-step}}:=\mathbf{S}_z\,B_{\mathrm{R}\to\mathrm{L}}$. In particular, $A_{\text{one-step,cl}}$ is the closed-loop matrix resulting from the LMI controller of the previous subsection and hence has its eigenvalues in the unit circle. In addition, $F_{\text{one-step}}:=\mathbf{S}_z\,F_{\mathrm{R}\to\mathrm{L}}$ and $F_{\mathrm{R}\to\mathrm{L}}\in\mathbb{R}^{25\times 2}$ is a *known* matrix to consider the effect of the *unknown* disturbance $d_k\in\mathcal{D}\subset\mathbb{R}^2$ on $\delta\bar{z}_k$, where $\mathcal{D}$ is a given polytope represented in terms of its vertices, i.e., $\mathcal{D}:=\mathrm{conv}\{d^1,\cdots,d^{n_{\mathcal{D}}}\}$ for some $n_{\mathcal{D}}>0$.

We now consider a force "pushing" the robot in the frontal plane and hence a 2-dimensional disturbance is considered for the roll angle and roll velocity. The results of this section can be extended to other kinds of disturbances. We assume that $d_k=d_0$ for $k=0$ and $d_k=0$ for $k\geq 1$. As mentioned previously, $B_{\mathrm{R}\to\mathrm{L}}\in\mathbf{B}_{\mathrm{R}\to\mathrm{L}}$. For a given time horizon $N\geq 1$, let

$$\mathbf{W}:=(w_0',\cdots,w_{N-1}')'\in\mathbb{R}^{pN}$$

be the vector of inputs to be determined. The *worst case* cost function is defined as

$$\begin{aligned}I_N(\delta\bar{z}_0,\mathbf{W}):=&\max_{d_0\in\mathcal{D},\,B_{\mathrm{R}\to\mathrm{L}}\in\mathbf{B}_{\mathrm{R}\to\mathrm{L}}}\Big\{\|P\,\delta\bar{z}_N\|_\infty\\&+\sum_{k=0}^{N-1}\|Q\,\delta\bar{z}_k\|_\infty+\|R\,w_k\|_\infty\Big\}\\ \delta\bar{z}_{k+1}=&\,A_{\text{one-step,cl}}\,\delta\bar{z}_k+B_{\text{one-step}}\,w_k+F_{\text{one-step}}\,d_k,\end{aligned} \tag{47}$$

where $P=P'>0$, $Q=Q'>0$ and $R=R'>0$. The cost function is then expressed as

$$\begin{aligned}&I_N^*(\delta\bar{z}_0):=\min_{\mathbf{W}}I_N(\delta\bar{z}_0,\mathbf{W})\\&\text{s.t.}\begin{cases}\delta\bar{z}_{k+1}=A_{\text{one-step,cl}}\,\delta\bar{z}_k+B_{\text{one-step}}\,w_k+F_{\text{one-step}}\,d_k\\ \|\kappa_{\mathrm{R}}(\bar{z}_0)-\beta_{\mathrm{R}}^*\|_\infty\leq\beta_{\max},\quad k=0,1,\cdots,N-1.\end{cases}\end{aligned} \tag{48}$$

We note that problem (47) looks for the worst value of the performance as a function of $\delta\bar{z}_0$ and $\mathbf{W}$. However, problem (48) can be expressed as a min-max problem and it minimizes the worst case cost function subject to feasibility of the input[11], i.e., $\|\kappa_{\mathrm{R}}(\bar{z}_0)-\beta_{\mathrm{R}}^*\|_\infty\leq\beta_{\max}$ for all possible disturbances $d_0\in\mathcal{D}$ and uncertainties $B_{\mathrm{R}\to\mathrm{L}}\in\mathbf{B}_{\mathrm{R}\to\mathrm{L}}$. In the min-max problem (48), $A_{\text{one-step,cl}}$ is assumed to be known. In particular, we approximate it by taking average of the vertices $\mathbf{S}_z\,A_{\mathrm{R}\to\mathrm{L},m}-\mathbf{S}_z\,B_{\mathrm{R}\to\mathrm{L},n}\,K_{\mathrm{R}}$ for $m=1,\cdots,n_{\mathcal{A}}$ and

[11]The approach is receding horizon, and hence we only implement $\kappa_{\mathrm{R}}(\bar{z}_0)$ at each event.

$n = 1, \cdots, n_{\mathcal{B}}$. This translates the problem (48) into a linear programming (LP) problem.

Remark 4: The LMI loop has already robustly stabilized the system to model uncertainty and hence variations in the A-matrix are not addressed here. The ROC loop is employed for disturbance rejection in the roll dynamics, and is being applied to an already stable system [35]. The LMI controller is linear, whereas the ROC controller is nonlinear, due to the saturation terms in (48). In the implementation of the two discrete-time controllers in Section VII, the practical advantages of separating their solutions will become clear.

To increase the basin of attraction, the input constraints on problem (48) have been expressed in terms of $\kappa_{\rm R}(\bar{z}_0) = \beta^*_{\rm R} - K_{\rm R}\,(\bar{z}_0 - z^*_{\rm R}) + w_0$ instead of w_0. To make this notion precise, we note that on the periodic orbit, the ground reaction forces are feasible. Large $\kappa_{\rm R}(\bar{z}_0)$ and thereby large changes in the piecewise-defined feedback law (12) for $\tau_i(q) \geq \tau_{\rm th}$ may result in infeasibility of the contact forces. Consequently, the positive scalar $\beta_{\max}$ in (48) has been introduced to enforce the stabilizing parameters to be in the feasible region.

Theorem 6 (Push Recovery as an LP problem): The push recovery problem against external disturbances is equivalent to an LP problem.

Proof: The performance

$$\mathcal{I}_N(\delta\bar{z}_0, \mathbf{W}, d_0, B_{\rm R\to L}) := \|P\,\delta\bar{z}_N\|_\infty + \sum_{k=0}^{N-1} \|Q\,\delta\bar{z}_k\|_\infty + \|R\,w_k\|_\infty$$

is convex with respect to $(d_0, B_{\rm R\to L})$ over the polyhedron $\mathcal{D}\times \mathbf{B}_{\rm R\to L}$. Based on results of [34], by introducing the scalar μ_0 as an upper bound for $\mathcal{I}_N$ and augmenting the variables of optimization by μ_0, the min-max problem (48) is equivalent to the following minimization problem on the augmented space

$$\begin{aligned} &\min_{\mathbf{W},\mu_0}\ \mu_0 \\ &\text{s.t.}\quad \mu_0 \geq \mathcal{I}_N(\delta\bar{z}_0, \mathbf{W}, d^l, B_{{\rm R\to L},n}),\ n = 1,\cdots,n_{\mathcal{B}} \\ &\qquad \|\kappa_{\rm R}(\bar{z}_0) - \beta^*_{\rm R}\|_\infty \leq \beta_{\max}, \qquad l = 1,\cdots,n_{\mathcal{D}}. \end{aligned} \tag{49}$$

Following the developments of [33], let μ^z_k and μ^w_k for $k = 0, 1, \cdots, N-1$ denote upper bounds for terms $\|Q\,\delta\bar{z}_k\|_\infty$ and $\|Rw_k\|_\infty$, respectively. In a similar manner μ^z_N is an upper bound to the term $\|P\delta\bar{z}_N\|_\infty$. Then, by defining

$$\boldsymbol{\mu} := (\mu_0, \mu^z_0, \cdots, \mu^z_N, \mu^w_0, \cdots, \mu^w_{N-1})' \in \mathbb{R}^{2N+2},$$

the optimization problem (49) is equivalent to the following LP problem on the augmented space

$$\begin{aligned} &\min_{\mathbf{W},\,\boldsymbol{\mu}}\ \mu_0 \\ &\text{s.t.}\ \begin{cases} \mu_0 \geq \mu^z_0 + \cdots + \mu^z_N + \mu^w_0 + \cdots + \mu^w_{N-1} \\ \mu^z_N\,\mathbf{1}_{25} \geq \pm P\,\delta\bar{z}_N(\delta\bar{z}_0; \mathbf{W}, d^l, B_{{\rm R\to L},n}) \\ \mu^z_k\,\mathbf{1}_{25} \geq \pm Q\,\delta\bar{z}_k(\delta\bar{z}_0; \mathbf{W}, d^l, B_{{\rm R\to L},n}) \\ \mu^w_k\,\mathbf{1}_p \geq \pm R\,w_k \\ \pm\kappa_{\rm R}(\bar{z}_0) \leq \beta_{\max}\,\mathbf{1}_p \mp \beta^*_{\rm R} \\ k = 0,1,\cdots,N-1,\ n = 1,\cdots,n_{\mathcal{B}},\ l = 1,\cdots,n_{\mathcal{D}}, \end{cases} \end{aligned} \tag{50}$$

where $\mathbf{1}_{25} := (1,\cdots,1)' \in \mathbb{R}^{25}$ and $\mathbf{1}_p := (1,\cdots,1)' \in \mathbb{R}^p$. Moreover, $\delta\bar{z}_k(\delta\bar{z}_0; \mathbf{W}, d^l, B_{{\rm R\to L},n})$ represents the solution of discrete-time system (46) when the input sequence is $\mathbf{W}$ and the Jacobian matrix $B_{\rm R\to L}$ and the disturbance d_0 are equal to the vertices $B_{{\rm R\to L},n}$ and d^l, respectively. ■

Remark 5 (Implementation of w_0): According to the one-step correction law developed in Theorem 4 and Remark 1, do the following steps at each discrete-time k.

Step (1) If $x \in \mathcal{T}_{\rm th,R}$ during the right stance phase, let $z = \pi_{\rm proj,R}(x)$ and $\delta z_0 = z - z^*_{\rm R}$. Next, solve the LP problem (50) for w_0 and employ

$$\beta_{\rm R} = \kappa_{\rm R}(z_0) = \beta^*_{\rm R} - K_{\rm R}\,\delta z_0 + w_0(\delta z_0) \tag{51}$$

for $\tau_{\rm R}(q) \geq \tau_{\rm th}$.

Step (2) If $x \in \mathcal{T}_{\rm th,L}$ during the left stance phase, set $z = \pi_{\rm proj,L}(x)$ and $\delta z_0 = \mathbf{S}_z\,z - z^*_{\rm R}$. Next, solve the LP problem (50) for w_0 and employ

$$\beta_{\rm L} = \mathbf{S}_\beta\,\kappa_{\rm R}(z_0) = \beta^*_{\rm L} - \mathbf{S}_\beta\,K_{\rm R}\,\delta z_0 + \mathbf{S}_\beta\,w_0(\delta z_0) \tag{52}$$

for $\tau_{\rm L}(q) \geq \tau_{\rm th}$.

VI. Application to the Hybrid Zero Dynamics

This section shows that the stability results of Sections IV and V can be applied to the feedback laws arising from virtual constraints and HZD. In particular, it is shown that the HZD-based hybrid controller satisfies hypotheses H1-H4. To present the main idea, associated with the stance phase $i \in \{\rm R, L\}$, define the following holonomic and parameterized output function to be regulated

$$y_i := h_i(q; \beta_{{\rm co},i}, \beta_i) := h_{c,i}(q) - h_{d,i}(\tau_i(q)) - h_{\rm co}(\tau_i(q); \beta_{{\rm co},i}) - h_{\rm st}(\tau_i(q); \beta_i). \tag{53}$$

In (53), $h_i(q; \beta_{{\rm co},i}, \beta_i)$ is a 6-dimensional output function which is parameterized by the corrective and stabilizing parameters $\beta_{{\rm co},i} \in \mathcal{B}_{{\rm co},i} \subset \mathbb{R}^{6\times n_{\rm co}}$ and $\beta_i \in \mathcal{B}_i \subset \mathbb{R}^{6\times n_{\rm st}}$ for $i \in \{\rm R, L\}$ and some $n_{\rm co}, n_{\rm st} > 0$. *Controlled variables*, denoted by $h_{c,i}(q)$, specify six independent holonomic quantities to be controlled. Furthermore, $h_{d,i}(\tau_i(q))$ represents the desired evolution of the controlled variables on the periodic orbit in terms of the strictly increasing quantity $\tau_i(q)$. In particular, $h_{c,i}(q) - h_{d,i}(\tau_i(q)) \equiv 0$ on the orbit $\mathcal{O}_i$. For later purposes, we define the *nominal output* function as $h_{{\rm nom},i}(q) := h_{c,i}(q) - h_{d,i}(\tau_i(q))$. Next, for the ATRIAS structure, $\tau_i(q)$ is chosen as the angle of the *virtual leg* with respect to the horizontal line to satisfy hypothesis H1, where the virtual leg is defined as the virtual line in the sagittal plane which connects the stance leg end to the hip joint. Moreover, it is assumed that the following hypothesis is satisfied for the nominal output function.

S1) There exists an output symmetry matrix $\mathbf{S}_h \in \mathbb{R}^{6\times 6}$ with the property $\mathbf{S}_h\,\mathbf{S}_h = I_{6\times 6}$ such that for every $q \in \mathcal{Q}$,

$$\begin{aligned} h_{c,\rm L}(q) &= \mathbf{S}_h\,h_{c,\rm R}(\mathbf{S}\,q) \\ h_{d,\rm L}(\tau_{\rm L}(q)) &= \mathbf{S}_h\,h_{d,\rm R}(\tau_{\rm R}(\mathbf{S}\,q)), \end{aligned} \tag{54}$$

which in turn implies that $h_{{\rm nom},\rm L}(q) = \mathbf{S}_h\,h_{{\rm nom},\rm R}(\mathbf{S}\,q)$ for all $q \in \mathcal{Q}$.

The functions $h_{\text{co}}(\tau_i(q);\beta_{\text{co},i})$ and $h_{\text{st}}(\tau_i(q);\beta_i)$ are referred to as the *corrective* and *stabilizing* terms, respectively, and they vanish on the periodic orbit. The corrective term is added to zero the output function (53) at the beginning of each step (i.e., hybrid invariance) and it is activated during the first half of the step. Following the developments of [36], it can be expressed as

$$h_{\text{co}}(\tau_i;\beta_{\text{co},i}) := \begin{cases} h_{\text{co}}^-(\tau_i;\beta_{\text{co},i}) & \text{if } \tau_i^+ \le \tau_i \le \tau_{\text{mid}} \\ 0_6 & \text{otherwise,} \end{cases} \tag{55}$$

where τ_i^+ and $\dot\tau_i^+$ are the initial values of τ_i and $\dot\tau_i$ on the current step, and $\tau_{\text{mid}} := \frac{1}{2}(\tau_i^+ + \tau_{\max})$. Here, we assume that the following hypothesis is satisfied.

S2) For $i \in \{\text{R},\text{L}\}$, $h_{\text{co}}^-(\tau_i;\beta_{\text{co},i})$ is $\mathcal{C}^2$ with respect to τ_i and linear in $\beta_{\text{co},i}$. In particular, $h_{\text{co}}^-(\tau_i;\mathbf{S}_h\,\beta_{\text{co},i}) = \mathbf{S}_h\,h_{\text{co}}^-(\tau_i;\beta_{\text{co},i})$.

Moreover, by defining $h_{\text{nom},i}^+$ and $\dot h_{\text{nom},i}^+$ as the initial values of the nominal output and its first time derivative at the beginning of the current step, $h_{\text{co}}^-(\tau_i;\beta_{\text{co},i})$ satisfies

$$\begin{aligned} &\text{(i) } h_{\text{co}}^-(\tau_i^+;\beta_{\text{co},i}) = h_{\text{nom},i}^+ \\ &\text{(ii) } \frac{\partial h_{\text{co}}^-}{\partial \tau_i}(\tau_i^+;\beta_{\text{co},i}) = \frac{\dot h_{\text{nom},i}^+}{\dot\tau_i^+} \\ &\text{(iii) } h_{\text{co}}^-(\tau_{\text{mid}};\beta_{\text{co},i}) = \frac{\partial h_{\text{co}}^-}{\partial \tau_i}(\tau_{\text{mid}};\beta_{\text{co},i}) = \frac{\partial^2 h_{\text{co}}^-}{\partial \tau_i^2}(\tau_{\text{mid}};\beta_{\text{co},i}) \\ &\qquad\qquad = 0_6 \end{aligned} \tag{56}$$

to create hybrid invariance (by (i) and (ii)) and to satisfy continuity of position, velocity and acceleration at $\tau_i = \tau_{\text{mid}}$ (by (iii)).

Next, we assume that the stabilizing term is activated over the second half of the step. The intuition behind this is that a human's push recovery is obtained by changing the step length at the end of the current step. In particular, we define

$$h_{\text{st}}(\tau_i;\beta_i) := \begin{cases} 0_6 & \text{if } \tau_i^+ \le \tau_i \le \tau_{\text{th}} \\ h_{\text{st}}^+(\tau_i;\beta_i) & \text{otherwise,} \end{cases} \tag{57}$$

for which the following hypothesis is satisfied,

S3) For $i \in \{\text{R},\text{L}\}$, $h_{\text{st}}^+(\tau_i;\beta_i)$ is $\mathcal{C}^2$ with respect to τ_i and linear in β_i. In particular, $h_{\text{st}}^+(\tau_i;\mathbf{S}_h\,\beta_i) = \mathbf{S}_h\,h_{\text{st}}^+(\tau_i;\beta_i)$.

Furthermore, we assume that $\tau_{\text{th}} > \tau_{\text{mid}}$ and

$$h_{\text{st}}^+(\tau_{\text{th}};\beta_i) = \frac{\partial h_{\text{st}}^+}{\partial \tau_i}(\tau_{\text{th}};\beta_i) = \frac{\partial^2 h_{\text{st}}^+}{\partial \tau_i^2}(\tau_{\text{th}};\beta_i) = 0_6 \tag{58}$$

to impose continuity of position, velocity and acceleration at $\tau_i = \tau_{\text{th}}$. Here, $\beta_{\text{co},i}$ is updated at the beginning of each step according to (56) and it remains constant during the step. The continuous-time feedback law is also obtained based on the standard input-output linearization, i.e.,

$$\begin{aligned} &\Gamma_i(x,\beta_{\text{co},i},\beta_i) = \\ &\quad -(L_{g_i}L_{f_i}y_i)^{-1}\left(L_{f_i}^2 y_i + \frac{K_D}{\epsilon}\,L_{f_i}y_i + \frac{K_P}{\epsilon^2}\,y_i\right), \end{aligned} \tag{59}$$

in which $K_P = k_p\,I_{6\times 6} > 0$, $K_D = k_d\,I_{6\times 6} > 0$ and $\epsilon > 0$ are controller parameters. In addition, (59) results in the output dynamics

$$\ddot y_i + \frac{K_D}{\epsilon}\,\dot y_i + \frac{K_P}{\epsilon^2}\,y_i = 0_6 \tag{60}$$

for which the origin $(y_i,\dot y_i) = (0_6,0_6)$ is exponentially stable.

Theorem 7: Let $\mathcal{O}$ be a symmetric and transversal periodic orbit for walking by ATRIAS. Assume that the ATRIAS model is symmetric with respect to the yz-plane of the torso frame and hypothesis H1 is met. Suppose further that assumptions S1-S3 together with (56) and (58) are fulfilled. Then, the feedback law (59) satisfies hypotheses H2-H4.

Proof: See Appendix B. ∎

Finally according to Theorem 7, the stabilizing parameters β_i in (53) can be updated by the one-step correction approach developed in Theorems 4, 5 and 6 and Remarks 1 and 5.

VII. Simulation Results

This section implements the work of the previous sections on two different simulation models of the bipedal robot ATRIAS 2.1, the hybrid model of Section II-E used for the controller design and a new model that assumes the walking surface is compliant and which explicitly computes the ground reaction forces acting on the robot. The second model will help us to investigate the robustness and sensitivity of the closed-loop system and simulation results against different modeling and integration approaches. In addition, the robustness of the robot in closed loop is evaluated against external forces acting as disturbances on the robot as well as parametric and nonparametric uncertainties in the model of walking. In particular, uncertainty in the yaw friction coefficient on the stance leg is considered.

A. Disturbance rejection

The purpose of this section is to show that the proposed control strategy will result in disturbance rejection against external forces acting on the robot. Here, an external *horizontal* force with a magnitude of $70(\text{N})$ (45% of the torso weight) is applied to the side of the robot to its COM; the disturbance is applied for 50% of duration of a step.

We consider a periodic orbit $\mathcal{O}$ with an average walking speed of $1.1(\text{m/s})$ for the hybrid model of walking. The continuous-time controller is based on the zero dynamics with the controlled variables during the right stance phase taken as

$$h_{c,\text{R}}(q) := \begin{bmatrix} \frac{1}{2}(q_{gr1\text{R}} + q_{gr2\text{R}}) \\ \frac{1}{2}(q_{gr1\text{L}} + q_{gr2\text{L}}) \\ q_{gr2\text{R}} - q_{gr1\text{R}} \\ q_{gr2\text{L}} - q_{gr1\text{L}} \\ q_{3\text{R}} \\ -x_{\text{cm}}(q) + \frac{1}{2}x_{\text{sw}}(q) \end{bmatrix}. \tag{61}$$

The first four outputs affect the sagittal plane motion of the robot, defining the angles of the legs with respect to the torso and the "knee bend". The fifth component is the stance hip angle. The sixth component is defined to keep the frontal plane component of the robot's COM between the stance and swing

legs. In particular, $x_{\rm cm}(q)$ and $x_{\rm sw}(q)$ denote the horizontal coordinates of the COM and swing leg end within the frontal plane[12]. We have observed that the first four components of the controlled variables in (61) can stabilize periodic orbits for the planar (i.e., 2D) model of ATRIAS [38]. The controlled variables during the left stance phase are defined according to Assumption S1 via $\mathbf{S}_h = \text{diag}\{1,1,1,1,1,-1\}$. The event-based control surface is defined at the $\frac{2}{3}$ point of the step, i.e., $\tau_{\rm th} = \frac{1}{3}\tau_{\min} + \frac{2}{3}\tau_{\max}$. Furthermore, the corrective and stabilizing terms are chosen as fifth and third order Bézier polynomials, respectively, to satisfy S2, S3, (56) and (58). Here the feasible set of perturbations to calculate the least square and two-point difference approximations for $A_{\rm R\to L}$ and $B_{\rm R\to L}$ are $\mathcal{E} = \{10^{-5}\times\{1,5\}, 10^{-4}\times\{1,5\}, 10^{-3}\times\{1:1:10\}\}$ and $\mathcal{E} = \{10^{-5}\times\{1,5\}, 10^{-4}\times\{1:1:10\}, 5\times10^{-3}, 10^{-2}\times\{1,1.5\}\}$, respectively. The three largest eigenvalues of the averaged Jacobian matrix

$$A_{\rm R\to R,ave} = \frac{1}{n_{\mathcal{A}}}\sum_{m=1}^{n_{\mathcal{A}}}(\mathbf{S}_z\, A_{{\rm R\to L},m})^2$$

are $\{1.1352, 1.000, 0.7241\}$. Due to the extensive variability in the numerical estimates of the Jacobian linearization of the Poincaré map, we tried designing a two-step DLQR controller for several pairs of two-step Jacobians $(A_{{\rm R\to R},m}, B_{{\rm R\to R},n})$ and all of them failed to bring the eigenvalues within the unit circle. We then tried a tedious iterative process, exhaustively searching over the collection of pairs $(A_{{\rm R\to R},m}, B_{{\rm R\to R},n})$ for a range of weights $\{Q_r\}_{r=1}^{M_Q}$ and $\{R_l\}_{l=1}^{M_R}$, solving for the DLQR gain. A two-step stabilizing gait was eventually found using this approach, but it had a small basin of attraction. In particular, this event-based action could only ensure stability for an external horizontal disturbance in the frontal plane with a magnitude of 15(N).

Due to lack of robust stability in the two-step approach and seeking a more robust solution, the one-step LMI problems of Theorem 5 are now solved through the `feasp` function of MATLAB for one-step Jacobians $(A_{{\rm R\to L},m}, B_{{\rm R\to L},n})$.

B. Preparing ROC controller for real-time implementation

In simulation, while the LP problem of Section V-B can be implemented as given, its solution is too slow for eventual real-time implementation. Hence, we present a real-time approach to employ the ROC. The LMI and ROC problems can be combined advantageously with the hybrid zero dynamics approach of Section VI. In this case, due to *hybrid invariance*, the state space of the corresponding discrete-time system will be reduced as the intersection of the 25-dimensional Poincaré section $\mathcal{T}_{{\rm th},i}, i\in\{\rm R,L\}$ and the 14-dimensional zero dynamics manifolds associated with the output functions. This intersection is 13-dimensional and referred to as the *restricted Poincaré section*. Next, we only update the stabilizing parameters for the first, second, and sixth components of the output function (53) and (61) (i.e., $p=3$ in (50)). In addition to these, we have observed that the roll dynamics are most important components of the 13-dimensional reduced-order discrete-time system in the optimal solutions of the min-max and equivalent LP problems. In this case, the corresponding state space for problems (48) and (50) is 2-dimensional which considers the evolution of the roll angle and velocity for which problem (50) has $10N+11$ inequality constraints[13], where N is the control horizon.

By gridding the state space and solving the optimization problem off-line for each grid point, the solutions of the LP problem (50) for the roll dynamics can be pre-computed and stored in a look-up table. Here, the state space is taken as $[-0.2\ 0.2]$(rad) $\times$ $[-2.5\ 2.5]$(rad/s) with 100×100 grids. Then, using Barycentric coordinates, the optimal solution w_0 can be interpolated in a linear manner. Furthermore, the parameters of the one-step ROC problem in Remark 5 are chosen as $N=2$, $P=Q=3\,I_{2\times2}$, $R=I_{3\times3}$, $\beta_{\max}=0.015$ and $\mathcal{D}=\text{conv}\{\pm d^1, \pm d^2\}$, where $d^1=(10,10)'$ and $d^2=(-10,10)'$.

The closed-loop simulation is started at the end of the left stance phase of the periodic orbit $\mathcal{O}$ and during the second step, a horizontal disturbance 70(N) is employed. Figures 2 and 3 present the phase portraits, plots of the ground reaction forces and the applied control inputs versus time as well as the norm of the discrete state $(q_{z\rm T}(k), q_{y\rm T}(k), \dot q_{y\rm T}(k), \dot q_{x\rm T}(k))'$ versus step number during 20 steps of walking. The push recovery and convergence to the periodic orbit is clear.

C. Robustness against parametric and nonparametric uncertainties

The objective of this section is to show that the proposed control strategies will result in stable walking motions even if the assumptions made in modeling of the hybrid system are not met exactly. In particular, we consider parametric and nonparametric uncertainties in the model of ATRIAS. To generate the periodic orbit for the nominal hybrid system, the stiffness and damping constants of the springs in the series elastic actuators were assumed to be $k_{\rm spring}=1200\,(\rm Nm/rad)$ and $k_{\rm damper}=70\,(\rm Nms/rad)$. Moreover, the coefficient $\gamma_{\rm friction}$ used in (3) to model the yaw friction about the stance leg end was assumed to be $100\,(\rm Nms/rad)$. The torso and robot masses are also 16.3 and 55 (kg), respectively [41]. Next, we consider -60%, $+25\%$, -20% and $+30\%$ parametric uncertainties in $\gamma_{\rm friction}$, $k_{\rm spring}$, $k_{\rm damper}$ and the torso mass, respectively. The impact model of Section II-D preserves the yaw motion about the swing leg end. Here, we relax this condition on the impact model as a nonparametric uncertainty. As another source of uncertainty, the term $L_{f_i}^2 y_i$ is removed from the continuous-time feedback law of (59) and hence, it is replaced by

$$\Gamma_i(x,\beta_{{\rm co},i},\beta_i) = -(L_{g_i}L_{f_i}y_i)^{-1}\Big(\frac{K_D}{\epsilon}\,L_{f_i}y_i + \frac{K_P}{\epsilon^2}\,y_i\Big), \tag{62}$$

which is a PD control action in which the inverse of the decoupling matrix (i.e., $(L_{g_i}L_{f_i}y_i)^{-1}$) can be considered as a scaling matrix. These changes to the system have several consequences. First, the effect of model parameters can be

[12]Here, we assume that the stance leg end defines the origin of the world frame.

[13]We remark that in this case, the LMI problems of Theorem 5 are still solved for the full-order (25-dimensional) Jacobian matrices.

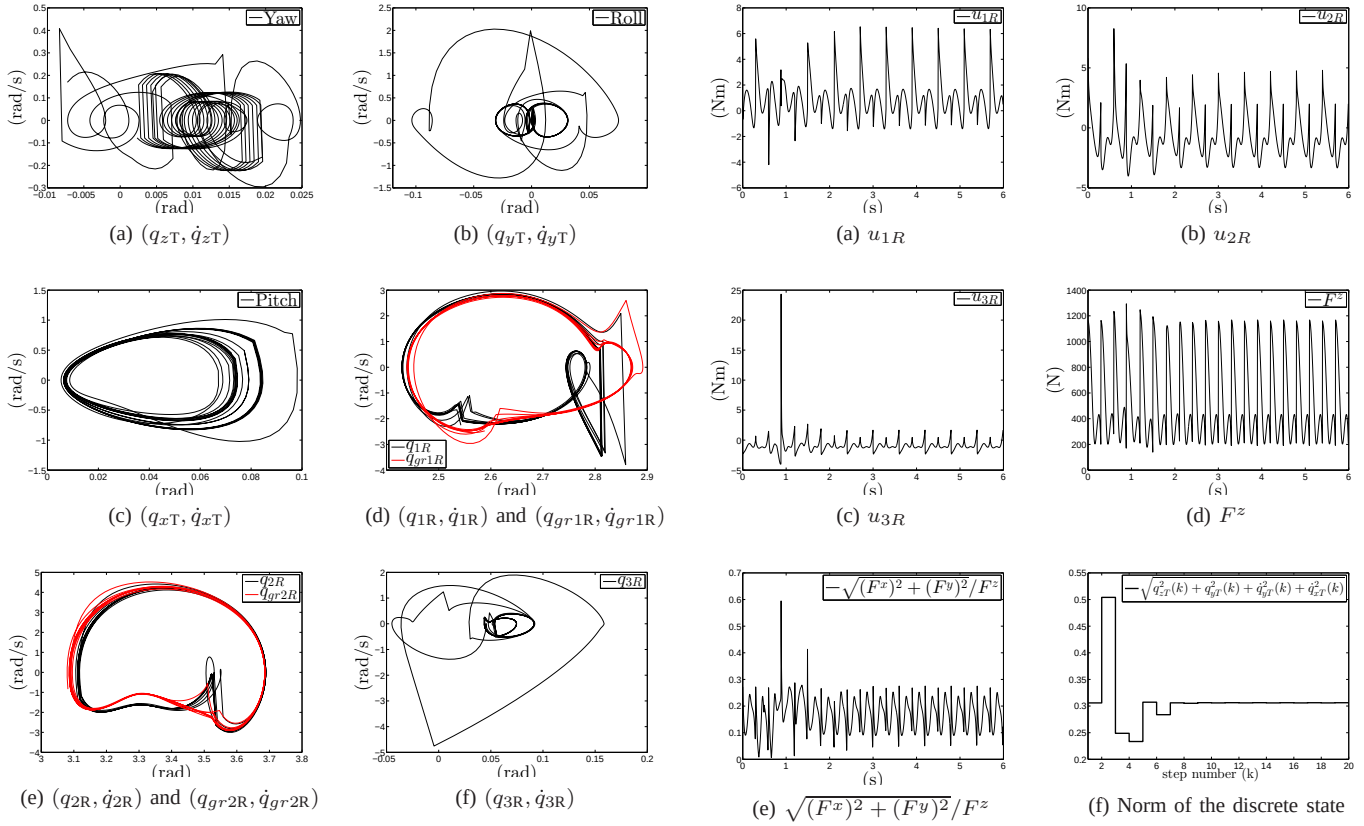

(a) $(q_{z\mathrm{T}}, \dot{q}_{z\mathrm{T}})$ (b) $(q_{y\mathrm{T}}, \dot{q}_{y\mathrm{T}})$ (c) $(q_{x\mathrm{T}}, \dot{q}_{x\mathrm{T}})$ (d) $(q_{1\mathrm{R}}, \dot{q}_{1\mathrm{R}})$ and $(q_{gr1\mathrm{R}}, \dot{q}_{gr1\mathrm{R}})$ (e) $(q_{2\mathrm{R}}, \dot{q}_{2\mathrm{R}})$ and $(q_{gr2\mathrm{R}}, \dot{q}_{gr2\mathrm{R}})$ (f) $(q_{3\mathrm{R}}, \dot{q}_{3\mathrm{R}})$

Fig. 2: Phase portraits for the closed-loop system during 20 consecutive steps of walking. During the second step, a horizontal force with the magnitude $70(\mathrm{N})$ is applied to the robot's COM over 50% of the gait.

(a) u_{1R} (b) u_{2R} (c) u_{3R} (d) F^z (e) $\sqrt{(F^x)^2+(F^y)^2}/F^z$ (f) Norm of the discrete state

Fig. 3: Plot of the control efforts, ground reaction forces and norm of the discrete state $(q_{z\mathrm{T}}(k), q_{y\mathrm{T}}(k), \dot{q}_{y\mathrm{T}}(k), \dot{q}_{x\mathrm{T}}(k))'$ for the closed-loop system during 20 consecutive steps of walking. During the second step, a horizontal force with the magnitude $70(\mathrm{N})$ is applied to the robot's COM over 50% of the gait.

investigated on the closed-loop behavior. Second, the effect of different impact models and continuous feedback laws is analyzed. Figure 4 shows the phase portraits during 50 consecutive steps of the closed-loop system when the robot is initialized at the left stance phase of the nominal orbit in the presence of all the above parametric and nonparametric uncertainties. According to Fig. 4, the robot's trajectory still converges to a limit cycle.

D. Robustness against different contact models

In Sections VII-A and VII-C, the evolution of the mechanical system was described by the hybrid model of walking given in (8), in which the impact forces are assumed to be impulses. In particular, the hybrid model considers right and left stance phases and corresponding impact maps; moreover, the velocity components of the state variables as well as ground reaction forces undergo a sudden change according to the instantaneous impact maps. This section presents a *continuous* and *compliant model* [40] to describe the evolution of the robot during all phases of walking including single support, impact, and double support.

The LuGre model [39] is used to represent forces between the contacting surfaces and can be integrated as an ordinary differential equation over time. This has several consequences. First, the evolution of the mechanical system subject to compliant ground reaction forces and non-instantaneous impact models can be assessed. In particular, the impact model is completely different from the one presented in Section II-D. Second, the robustness of the closed-loop system to different models of the ground is analyzed. In addition to these, parameter uncertainty (in particular, in the yaw friction coefficient) will be introduced in the robot model. Third, using this compliant simulator, we can model dynamic walking with *passive prosthetic feet.* ATRIAS is capable of being fitted with nontrivial feet which is another source of nonparametric uncertainty. The compliant model uses the floating-base or flight-phase model of the robot. By augmenting the configuration variables $q \in \mathcal{Q}$ by the position vector of the base of the torso link, the 16-dimensional flight-phase coordinate vector can be expressed as $q_f := (x_{\mathrm{T}}, y_{\mathrm{T}}, z_{\mathrm{T}}, q')' \in \mathbb{R}^3 \times \mathcal{Q}$, in which $(x_{\mathrm{T}}, y_{\mathrm{T}}, z_{\mathrm{T}})' \in \mathbb{R}^3$ denotes the position of the base of the torso link with respect to the world frame. Next, the evolution of the mechanical system subject to the contact forces can be

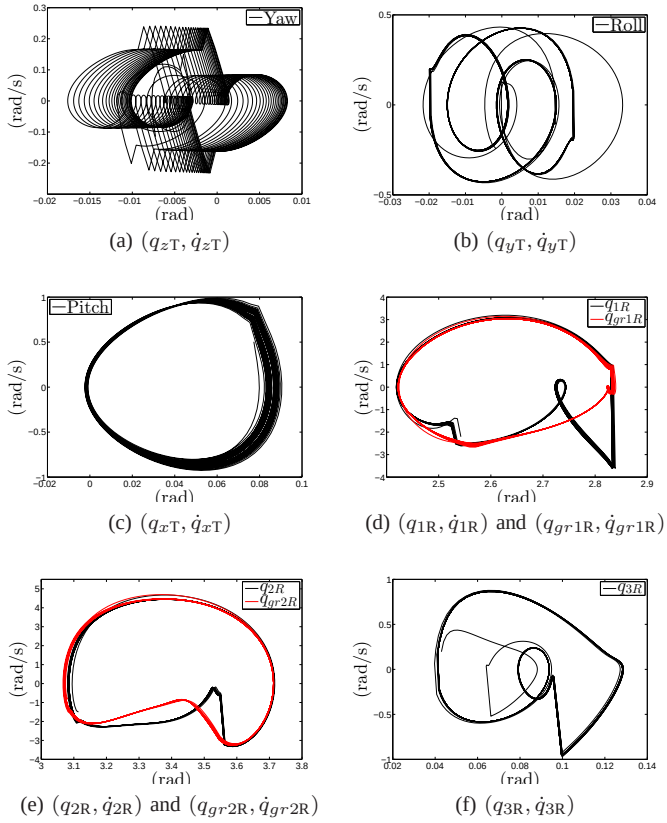

(a) $(q_{z\mathrm{T}}, \dot{q}_{z\mathrm{T}})$ (b) $(q_{y\mathrm{T}}, \dot{q}_{y\mathrm{T}})$

(c) $(q_{x\mathrm{T}}, \dot{q}_{x\mathrm{T}})$ (d) $(q_{1\mathrm{R}}, \dot{q}_{1\mathrm{R}})$ and $(q_{gr1\mathrm{R}}, \dot{q}_{gr1\mathrm{R}})$

(e) $(q_{2\mathrm{R}}, \dot{q}_{2\mathrm{R}})$ and $(q_{gr2\mathrm{R}}, \dot{q}_{gr2\mathrm{R}})$ (f) $(q_{3\mathrm{R}}, \dot{q}_{3\mathrm{R}})$

Fig. 4: Phase portraits for the closed-loop system with parametric and nonparametric uncertainties during 50 consecutive steps of walking.

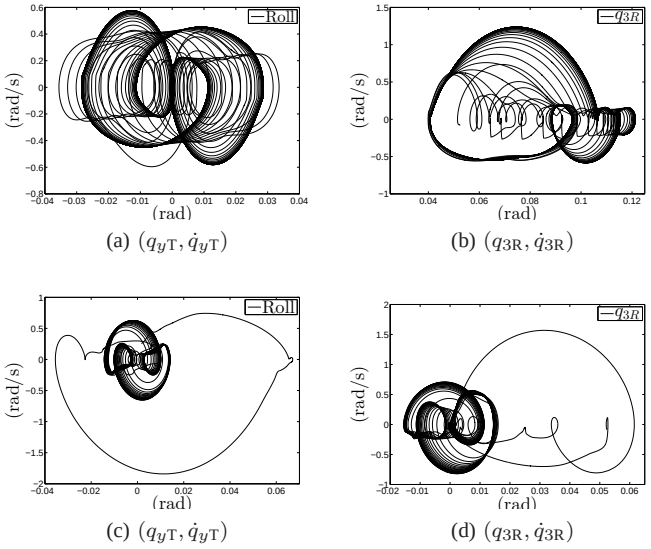

(a) $(q_{y\mathrm{T}}, \dot{q}_{y\mathrm{T}})$ (b) $(q_{3\mathrm{R}}, \dot{q}_{3\mathrm{R}})$

(c) $(q_{y\mathrm{T}}, \dot{q}_{y\mathrm{T}})$ (d) $(q_{3\mathrm{R}}, \dot{q}_{3\mathrm{R}})$

Fig. 5: Roll and hip phase portraits for the compliant model with parametric and nonparametric uncertainties during walking with point feet (Figs. 5a and 5b) and passive prosthetic feet (Figs. 5c and 5d).

expressed as

$$D_f(q_f)\,\ddot{q}_f + H_f(q_f, \dot{q}_f) = B_f\,u + \sum_{l\in\{\text{contac points}\}} \frac{\partial p_l}{\partial q_f}'(q_f)\,\lambda_l + \sum_{l\in\{\text{contac points}\}} \text{yaw friction term at contact point } l, \tag{63}$$

where $D_f(q_f) \in \mathbb{R}^{16\times 16}$ and $B_f \in \mathbb{R}^{16\times 6}$ represent the flight-phase mass-inertia and input matrices, respectively. Moreover, $H_f(q_f, \dot{q}_f) \in \mathbb{R}^{16}$ denotes the corresponding Coriolis, centrifugal, gravity, spring and damper forces. Next, $p_l \in \mathbb{R}^3$ is the Cartesian coordinates of the contact point l. In addition, $\lambda_l := (\lambda_l^x, \lambda_l^y, \lambda_l^z)' \in \mathbb{R}^3$ represents the forces acting on the point l being given by the compliant, nonlinear and dynamic ground model of [40], [39]. Moreover, the third term on the right-hand side of (63) uses the principle of the virtual work to represent the yaw friction term of (3), which is active when point l is in contact with the ground.

In the simulation, we consider -80% and -40% parametric uncertainties in γ_{friction} (i.e., yaw friction coefficient) and spring damping ratio, respectively. In addition to these parametric uncertainties, the PD feedback law of (62) is employed. Figures 5a and 5b depict the roll and right hip phase portraits for the closed-loop compliant model with point feet. The phase portraits for walking with prosthetic feet and zero yaw friction coefficient have been presented in Figures 5c and 5d. Here, the initial condition is taken at the end of the right stance phase on the nominal trajectory and it can be seen that the asymptotically stable limit cycle of the nominal closed-loop system seems to persist in the presence of compliant forces and uncertainties.

VIII. Conclusion

This paper has presented a time-invariant and one-step event-based controller, on the basis of left-right symmetry, for robust stabilization of periodic orbits for 3D bipedal walking against external disturbances as well as parametric and nonparametric uncertainty. The results have been illustrated on a simulation model of ATRIAS 2.1 a highly underactuated 3D bipedal robot with point feet and series-compliant actuators.

The Poincaré return maps for 3D walking and running locomotion naturally consist of the robot's dynamics over two steps, that is, they include locomotion on both the left and right legs. It follows that event-based controllers designed on the basis of the Poincaré return map will update parameters in a two-step manner, that is, once every two steps of the robot. Factorization of these Poincaré return maps into the right-to-left and left-to-right maps results in a periodically time-varying discrete-time system with period-2. This approach leads to a periodically time-varying one-step controller design problem. Next, due to the existence of the large springs used in series-compliant actuators for energy efficiency and light legs, there is a wide range of time scales in the underlying continuous dynamics. This yields inaccuracies in the Jacobians matrices of the Poincaré maps which are calculated using numerical differentiation algorithms based on a set of perturbation values. Additional uncertainty on the Poincaré section may arise

because of parametric and nonparametric uncertainties in the model and external disturbances acting on the robot.

Regarding the parametric uncertainties corresponding to a family of linear models rising from a set of perturbation values, the paper presented a robust one-step event-based controller consisting of two loops. The first loop employs a robust static update law for the Poincaré maps against numerical and parametric uncertainties. In particular, the paper presented a robust control formalism whereby a convex set of approximations to the Jacobian linearization is generated and a stabilizing controller is designed through a set of LMIs. The second loop of the discrete action updates the parameters to optimize the worst case performance, while considering the saturation of the discrete-time controller for all possible disturbances and polyhedral parametric uncertainties in the Poincaré return maps. Finally, the paper extended the analytical results to feedback laws arising from virtual constraints and HZD as special members of this general class.

In future work, the results of the paper will be implemented on the ATRIAS robot. It would be very interesting to develop one-step robust and stabilizing update laws without considering the symmetry structure in the Poincaré analysis. In addition, this can help us to develop a set of multiple Poincaré sections and the corresponding event-based update policies within each step to stabilize periodic orbits of walking.

APPENDIX A
PROOF OF THEOREM 1

Part (1): Let $\mathcal{K}_{\rm R}(q,\dot q) := \frac{1}{2}\dot q'\, D_{\rm R}(q)\,\dot q$, $\mathcal{K}_{\rm L} := \frac{1}{2}\dot q'\, D_{\rm L}(q)\,\dot q$, $\mathcal{V}_{\rm R}(q)$ and $\mathcal{V}_{\rm L}(q)$ denote the kinetic and potential energies, corresponding to the gravity, for ATRIAS during the right and left stance phases, respectively. Symmetry in the robot's structure implies the invariance of the kinetic energy under the $\mathbf{S}$ action, i.e., $\mathcal{K}_{\rm L}(q,\dot q) = \mathcal{K}_{\rm R}(\mathbf{S}\,q, \mathbf{S}\,\dot q)$ for every $(q',\dot q')' \in T\mathcal{Q}$, which in turn results in $D_{\rm L}(q) = \mathbf{S}'\, D_{\rm R}(\mathbf{S}\,q)\,\mathbf{S}$. This latter fact together with the formula of the $(k,j)^{th}$ element of the Coriolis matrix, i.e.,

$$c_{kj} = \frac{1}{2}\sum_{i=1}^{13}\Big(\frac{\partial d_{kj}}{\partial q_i} + \frac{\partial d_{ki}}{\partial q_j} - \frac{\partial d_{ij}}{\partial q_k}\Big)\,\dot q_i$$

implies that $C_{\rm L}(q,\dot q) = \mathbf{S}'\, C_{\rm R}(\mathbf{S}\,q, \mathbf{S}\,\dot q)\,\mathbf{S}$. Furthermore, the invariance of the potential energy under the $\mathbf{S}$ action, i.e., $\mathcal{V}_{\rm L}(q) = \mathcal{V}_{\rm R}(\mathbf{S}\,q)$, results in $G_{\rm L}(q) = \mathbf{S}'\, G_{\rm R}(\mathbf{S}\,q)$. Similar result for the potential energy of the springs yields $K_{\text{spring}}\, q = \mathbf{S}'\, K_{\text{spring}}\,\mathbf{S}\,q$. In an analogous manner, $K_{\text{damper}}\,\dot q = \mathbf{S}'\, K_{\text{damper}}\,\mathbf{S}\,\dot q$. In addition, if we define $\mathbf{S}_\omega := -1$ to consider the symmetry for the angular velocity corresponding to the yaw at the leg ends, then $\omega^z_{f\rm L}(q,\dot q) = \mathbf{S}_\omega\,\omega^z_{f\rm R}(\mathbf{S}\,q, \mathbf{S}\,\dot q)$ which in turn yields $E^z_{f\rm L}(q) = \mathbf{S}_\omega\, E^z_{f\rm R}(\mathbf{S}\,q)\,\mathbf{S}$ for all $(q',\dot q')' \in T\mathcal{Q}$. These facts imply that $H_{\rm L}(q,\dot q) = \mathbf{S}'\, H_{\rm R}(\mathbf{S}\,q, \mathbf{S}\,\dot q)$.

Part (2): During the impact, we assume that the stance leg end is on the origin of the world frame. Since the impact map is obtained based on the extended model, we first define the symmetry matrix for the extended model as $\mathbf{S}_e \in \mathbb{R}^{16\times 16}$ by $\mathbf{S}_e := \text{block diag}\{\mathbf{S}, \mathbf{S}_p\}$, where $\mathbf{S}_p := \text{diag}\{-1,1,1\}$ is the *position symmetry matrix* to consider symmetry for the Cartesian coordinates of the leg end during walking along the y-axis of the world frame. In addition, we define the *position-angular velocity symmetry matrix* as $\mathbf{S}_{p\omega} := \text{bolck diag}\{\mathbf{S}_p, \mathbf{S}_\omega\} \in \mathbb{R}^{4\times 4}$. Using these definitions, (7) and the chain rule, it can be concluded that

$$E_{f\rm L,e}(q_e) = \mathbf{S}_{p\omega}\, E_{f\rm R,e}(\mathbf{S}_e\, q_e)\,\mathbf{S}_e, \tag{64}$$

for every $q_e \in \mathcal{Q}_e$, where $E_{f\rm L,e}$ is the extension of (7) for the left leg in the coordinates $(q', p'_{f\rm R})'$. According to (6), let us define

$$\Upsilon_{\rm R\to L}(q_e^-) := \begin{bmatrix} D_{e,\rm R}(q_e^-) & -E'_{f\rm L,e}(q_e^-) \\ E_{f\rm L,e}(q_e^-) & 0_{4\times 4}\end{bmatrix}^{-1}\begin{bmatrix} D_{e,\rm R}(q_e^-) \\ 0_{4\times 16}\end{bmatrix}$$

and

$$\Upsilon_{\rm L\to R}(q_e^-) := \begin{bmatrix} D_{e,\rm L}(q_e^-) & -E'_{f\rm R,e}(q_e^-) \\ E_{f\rm R,e}(q_e^-) & 0_{4\times 4}\end{bmatrix}^{-1}\begin{bmatrix} D_{e,\rm L}(q_e^-) \\ 0_{4\times 16}\end{bmatrix},$$

where $D_{e,\rm R}$ and $D_{e,\rm L}$ are mass-inertia matrices for the extended model in the coordinates $(q', p'_{f\rm R})'$ and $(q', p'_{f\rm L})'$, respectively. Similar to the proof of Part (1), it can be shown that $D_{e,\rm L}(q_e) = \mathbf{S}'_e\, D_{e,\rm R}(\mathbf{S}_e\, q_e)\,\mathbf{S}_e$ for every $q_e \in \mathcal{Q}_e$. This property together with (64) and straightforward calculations imply that for every $q_e^- \in \mathcal{Q}_e$, $\Upsilon_{\rm L\to R}(q_e^-) = \text{block diag}\{\mathbf{S}_e, \mathbf{S}_{p\omega}\} \times \Upsilon_{\rm R\to L}(\mathbf{S}_e\, q_e^-)\,\mathbf{S}_e$ which in turn completes the proof for the impact model (6).

APPENDIX B
PROOF OF THEOREM 7

Since (i) the nominal output function $h_{\text{nom},i}(q)$ together with the corrective and stabilizing terms vanishes on the orbit $\mathcal{O}_i$ and (ii) from S2 and S3, $h^-_{\text{co}}(\tau_i;\beta_{\text{co},i})$ and $h^+_{\text{st}}(\tau_i;\beta_i)$ are linear in $\beta_{\text{co},i}$ and β_i, it can be concluded that on the periodic orbit $\mathcal{O}$, the corrective and stabilizing parameters are zero, i.e., $\beta^*_{\text{co},i} = 0_{6\times n_{\text{co}}}$ and $\beta^*_i = 0_{6\times n_{\text{st}}}$. Next, according to the construction procedure of the output functions in (56) and (58) and $\tau_{\text{th}} > \tau_{\text{mid}}$, hypotheses H2 and H3 are satisfied for the nominal parameters $\beta^*_{\text{co},i}$ and β^*_i.

During phase $i \in \{\rm R, L\}$, the output dynamics (60) can be rewritten as

$$\frac{\partial h_i}{\partial q}(q;\beta_{\text{co},i},\beta_i)\, D_i^{-1}(q)\, B\,\Gamma_i(x,\beta_{\text{co},i},\beta_i) = \eta_i(x,\beta_{\text{co},i},\beta_i), \tag{65}$$

in which

$$\eta_i(x,\beta_{\text{co},i},\beta_i) := \frac{\partial h_i}{\partial q}\, D_i^{-1}\, H_i - \frac{\partial}{\partial q}\Big(\frac{\partial h_i}{\partial q}\,\dot q\Big)\,\dot q - \frac{K_D}{\epsilon}\,\frac{\partial h_i}{\partial q}\,\dot q - \frac{K_P}{\epsilon^2}h_i. \tag{66}$$

Furthermore, assumptions S1-S3 imply that

$$h_{\rm L}(q;\beta_{\text{co,L}},\beta_{\rm L}) = \mathbf{S}_h\, h_{\rm R}(\mathbf{S}\,q; \mathbf{S}_h\,\beta_{\text{co,L}}, \mathbf{S}_h\,\beta_{\rm L}). \tag{67}$$

This latter fact together with Part (1) of Theorem 1 yields

$$\begin{aligned}\eta_{\rm L}(x,\beta_{\text{co,L}},\beta_{\rm L}) &= \mathbf{S}_h\,\eta_{\rm R}(\bar{\mathbf{S}}\,x, \mathbf{S}_h\,\beta_{\text{co,L}}, \mathbf{S}_h\,\beta_{\rm L}) \\ \frac{\partial h_{\rm L}}{\partial q}(q;\beta_{\text{co,L}},\beta_{\rm L})\, D_{\rm L}^{-1}(q)\, B &= \mathbf{S}_h\,\frac{\partial h_{\rm R}}{\partial q}(\mathbf{S}\,q; \mathbf{S}_h\,\beta_{\text{co,L}}, \mathbf{S}_h\,\beta_{\rm L}) \\ &\quad\times D_{\rm R}^{-1}(\mathbf{S}\,q)\, B.\end{aligned} \tag{68}$$

Finally, considering (65) and (68), it can be concluded that

$$B\,\Gamma_{\mathrm{L}}(x,\beta_{\mathrm{co,L}},\beta_{\mathrm{L}}) = \mathbf{S}'\,B\,\Gamma_{\mathrm{R}}(\bar{\mathbf{S}}\,x,\mathbf{S}_h\,\beta_{\mathrm{co,L}},\mathbf{S}_h\,\beta_{\mathrm{L}})$$

which completes the proof[14].

ACKNOWLEDGMENT

The authors would like to thank Kevin Galloway for his valuable contributions to the compliant model of ATRIAS 2.1.

REFERENCES

[1] J. A. Grimes and J. W. Hurst, "The design of ATRIAS 1.0 a unique monoped, hopping robot," *Proceedings of the 2012 International Conference on Climbing and walking Robots and the Support Technologies for Mobile Machines*, Baltimore, MD, pp. 548-554, July 2012.

[2] A. Ramezani and J. W. Grizzle, "ATRIAS 2.0, a new 3D bipedal robotic walker and runner," *Proceedings of the 2012 International Conference on Climbing and walking Robots and the Support Technologies for Mobile Machines*, Baltimore, MD, pp. 467-474, July 2012.

[3] D. D. Bainov and P. S. Simeonov, *Systems with Impulse Effects: Stability, Theory and Applications*, Ellis Horwood Limited, April 1989.

[4] H. Ye, A. N. Michel, and L. Hou, "Stability theory for hybrid dynamical systems," *IEEE Transactions on Automatic Control*, vol. 43, no. 4, pp. 461-474, 1998.

[5] J. W. Grizzle, G. Abba, and F. Plestan, "Asymptotically stable walking for biped robots: Analysis via systems with impulse effects," *IEEE Transactions on Automatic Control*, vol. 46, issue 1, pp. 51-64, January 2001.

[6] E. R. Westervelt, J. W. Grizzle, C. Chevallereau, J. H. Choi, and B. Morris, *Feedback Control of Dynamic Bipedal Robot Locomotion*, Boca Raton: CRC Press, June 2007.

[7] A. D. Ames, R. Sinnet and E. Wendel, "Three-dimensional kneed bipedal walking: A hybrid geometric approach," *Proceedings of the 12th International Conference on Hybrid Systems: Computation and Control, Lecture Notes in Computer Science (HSCC 2009)*, vol. 5469, pp. 16-30, April 2009.

[8] J. W. Grizzle, C. Chevallereau, A. D. Ames, and R. W. Sinnet, "3D bipedal robotic walking: Models, feedback control, and open problems," *Proceedings of the IFAC Symposium on Nonlinear Control Systems*, Bologna, September 2010.

[9] M. W. Spong and F. Bullo, "Controlled symmetries and passive walking," *IEEE Transactions on Automatic Control*, vol. 50, no. 7, pp. 1025-1031, July 2005.

[10] G. Song and M. Zefran, "Underactuated dynamic three-dimensional bipedal walking," *Proceedings of the IEEE International Conference on Robotics and Automation*, Orlando, FL: IEEE Press, pp. 854-859, May 2006.

[11] T. Fukuda, M. Doi, Y. Hasegawa, and H. Kajima, "Multi-locomotion control of biped locomotion and brachiation robot," in *Fast Motions in Biomechanics and Robotics* (Lecture Notes in Control and Information Sciences), Heidelberg, Germany: Springer-Verlag, 2006, pp. 121-145.

[12] K. Akbari Hamed, N. Sadati, W. A. Gruver, and G. A. Dumont, "Stabilization of periodic orbits for planar walking with non-instantaneous double support phase," *IEEE Transactions on Systems, Man, and Cybernetics, Part A*, vol. 42, issue 3, pp. 685-706, May 2012.

[13] I. R. Manchester, U. Mettin, F. Iida, and R. Tedrake, "Stable dynamic walking over uneven terrain," *Interntaional Journal of Robotics Research*, vol. 30, no. 3, pp. 265-279, 2011.

[14] R. D. Gregg, A. K. Tilton, S. Candido, T. Bretl, and M. W. Spong, "Control and planning of 3-D dynamic walking with asymptotically stable gait primitives," *IEEE Transactions on Robotics*, vol. 28, no. 6, pp. 1415-1423, December 2012.

[15] R. D. Gregg and M. W. Spong, "Reduction-based control of three-dimensional bipedal walking robots," *International Journal of Robotics Research*, vol. 26, no. 6, pp. 680-702, 2010.

[14]In particular, by defining the augmented state vector including the states of the mechanical system together with the corrective parameters, we can define a closed-loop deadbeat hybrid extension of the hybrid model for which Remarks 7 and 8 of [36] are satisfied. Next, this together with the symmetry in the augmented model helps us to extend the results developed in Theorems 4, 5 and 6 and Remarks 1 and 5 for the hybrid extension of the model.

[16] J. K. Holm, D. Lee, and M. W. Spong, "Time-scaling trajectories of passive-dynamic bipedal robots," *Proceedings of the IEEE International Conference of Robotics & Automation*, Roma, Italy, 2007, pp. 3603-3608.

[17] H. Dai and R. Tedrake, "Optimizing robust limit cycles for legged locomotion on unknown terrain," *Proceedings of the 51st IEEE International Conference on Decision and Control*, Maui, Hawaii, pp. 1207-1213, December, 2012.

[18] R. Tedrake, T. W. Zhang, and H. S. Seung, "Stochastic policy gradient reinforcement learning on a simple 3D biped," *Proceedings of the IEEE International Conference on Intelligent Robots and Systems*, Sendai, Japan, September 2004.

[19] V. I. Arnold, *Geometrical Methods in the Theory of Ordinary Differential Equations*, Springer-Verlag, 1988.

[20] T. S. Parker and L. O. Chua, *Practical Numerical Algorithms for Chaotic Systems*, Springer-Verlag, New York, 1989.

[21] W. M. Haddad and V. Chellaboina, *Nonlinear Dynamical Systems and Control: A Lyapunov-Based Approach*, Princeton, NJ, Princeton University Press, 2008.

[22] E. R. Westervelt, J. W. Grizzle, and C. Canudas, "Switching and PI control of walking motions of planar biped walkers," *IEEE Transactions on Automatic Control*, vol. 48, issue 2, pp. 308-312, February 2003.

[23] J. W. Grizzle, "Remarks on event-based stabilization of periodic orbits in systems with impulse effects," *Second International Symposium on Communications, Control and Signal Processing*, 2006.

[24] E. R. Westervelt, G. Buche, and J. W. Grizzle, "Experimental validation of a framework for the design of controllers that induce stable walking in planar bipeds," *The International Journal of Robotics Research*, vol. 24, no. 6, pp. 559-582, June 2004.

[25] K. Sreenath, H. W. Park, J. W. Grizzle, "Design and experimental implementation of a compliant hybrid zero dynamics controller with active force control for running on MABEL," *Proceedings of the 2012 IEEE International Conference on Robotics and Automation*, Saint Paul, MN, pp. 51-56, May 2012.

[26] C. Chevallereau, J. W. Grizzle, and C. L. Shih, "Asymptotically stable walking of a five-link underactuated 3-D bipedal robot," *IEEE Transactions on Robotics*, vol. 25, issue 1, pp. 37-50, February 2009.

[27] K. Akbari Hamed, N. Sadati, W. A. Gruver, and G. A. Dumont, "Exponential stabilisation of periodic orbits for running of a three-dimensional monopedal robot," *IET Control Theory & Applications*, vol. 5, issue 11, pp. 1304-1320, 2011.

[28] C. L. Shih, J. W. Grizzle, and C. Chevallereau, "From stable walking to steering of a 3D bipedal robot with passive point feet," *Robotica*, vol 30, issue 7, pp. 1119-1130, 2012.

[29] K. Akbari Hamed and J. W. Grizzle, "Robust event-based stabilization of periodic orbits for hybrid systems: Application to an underactuated 3D bipedal robot," *Proceedings of the 2013 American Control Conference*, Washington, DC, pp. 6206-6212, June 2013.

[30] Y. Hürmüzlü and D. B. Marghitu, "Rigid body collisions of planar kinematic chains with multiple contact points," *International Journal of Robotics Research*, vol. 13, issue 1, pp. 82-92, 1994.

[31] R. M. Murray, Z. Li, and S. Shankar Sastry, *A Mathematical Introduction to Robotic Manipulation*, Boca Raton: CRC Press, 1994.

[32] M. C. de Oliveira, J. Bernussou, and J. C. Geromel, "A new discrete-time robust stability condition," *Systems & Control Letters*, vol. 37, pp. 261-265, 1999.

[33] P. J. Campo and M. Morari, "Model predictive optimal averaging level control," AIChE Journal, vol. 35, issue 4, pp. 579-591, 1989.

[34] F. Borrelli, A. Bemporad, and M. Morari, *Predictive control for linear and hybrid systems*, Cambridge University Press, 2011, In press.

[35] L. Magni and R. Scattolini, "Robustness and robust design of MPC for nonlinear discrete-time systems," *Assessment and Future Directions of Nonlinear Model Predictive Control*, Lecture Notes in Control and Information Sciences, vol. 358, 2007, pp. 239-254.

[36] B. Morris and J. W. Grizzle, "Hybrid invariant manifolds in systems with impulse effects with application to periodic locomotion in bipedal robots," *IEEE Transactions on Automatic Control*, vol. 54, issue 8, pp. 1751-1764, August 2009.

[37] C. Canudas, B. Siciliano, and G. Bastin, *Theory of Robot Control*, Springer-Verlag, London, 1996.

[38] A. Ramezani, J. W. Hurst, K. Akbari Hamed, and J. W. Grizzle, "Performance analysis and feedback control of ATRIAS, a 3D bipedal robot," *Journal of Dynamic Systems, Measurement, and Control*, accepted to appear, September 2013.

[39] C. Canudas de Wit, H. Olsson, K. J. Astrom, and P. Lischinsky, "A new model for control of systems with friction," *IEEE Transactions on Automatic Control*, vol. 40, no. 3, March 1995.

[40] F. Plestan, J. W. Grizzle, E. R. Westervelt, and G. Abba, "Stable walking of a 7-DOF biped robot," *IEEE Transactions on Robotics and Automation*, vol. 19, issue 4, pp. 653-668, August 2008.
[41] https://sites.google.com/site/atrias21/

Kaveh Akbari Hamed was born in Tabriz, Iran. He received the B.S. degree in electrical engineering from the University of Tabriz, Iran in 2004 and the M.S. and Ph.D. degrees in electrical engineering (Control Engineering) from Sharif University of Technology, Tehran, Iran in 2006 and 2011, respectively. He is currently a postdoctoral research fellow at the Electrical Engineering and Computer Science Department of the University of Michigan, Ann Arbor, MI, USA. His research interests have been focused on nonlinear and robust control, robotics, dynamical legged locomotion, hybrid systems, and optimization.

Jessy W. Grizzle received the Ph.D. in electrical engineering from The University of Texas at Austin in 1983 and in 1984 held an NSF-NATO Postdoctoral Fellowship in Science in Paris, France. Since September 1987, he has been with The University of Michigan, Ann Arbor, where he is the Jerry and Carol Levin Professor of Engineering. He jointly holds sixteen patents dealing with emissions reduction in passenger vehicles through improved control system design. Professor Grizzle is a Fellow of the IEEE and of IFAC. He received the Paper of the Year Award from the IEEE Vehicular Technology Society in 1993, the George S. Axelby Award in 2002, the Control Systems Technology Award in 2003, and the Bode Lecture in 2012. His work on bipedal locomotion has been the object of numerous plenary lectures and has been featured in The Economist, Wired Magazine, Discover Magazine, Scientific American, Popular Mechanics and several television programs.